

SYSTEM RELIABILITY OF STRUCTURAL STEEL FRAMES: COMPONENT- AND SYSTEM-BASED DESIGN METHODS

Damir Akchurin^{1, †}, Sándor Ádány^{2, 3}, Ronald D. Ziemian⁴, Kim J. R. Rasmussen⁵, Benjamin W. Schafer⁶

¹Graduate Research Assistant, Department of Civil and Systems Engineering, Johns Hopkins University, Baltimore, MD, USA

²Associate Research Scientist, Department of Civil and Systems Engineering, Johns Hopkins University, Baltimore, MD, USA

³Professor, Department of Structural Mechanics, Budapest University of Technology and Economics, Budapest Hungary

⁴Professor, Department of Civil and Environmental Engineering, Bucknell University, Lewisburg, PA, USA

⁵Professor, School of Civil Engineering, University of Sydney, Sydney, NSW, Australia

⁶Professor, Department of Civil and Systems Engineering, Johns Hopkins University, Baltimore, MD, USA

[†]Corresponding author, akchurd1@jhu.edu

ABSTRACT

Current design practice for structural steel buildings is largely governed by component-based design methods, which ensure strength and reliability on the level of individual components of a structural system. However, with the recent advances and increasing accessibility of structural modeling and analysis tools, there has been a growing interest in system-based design methods, which ensure strength and reliability on the level of the entire structural system. As the profession moves toward broader adoption of system-based design methods, additional studies are essential to quantify system-level reliabilities and inform future design codes. In this study, we investigate system-level reliabilities achieved by two component-based design methods, Direct Analysis Method and Advanced Elastic Analysis Method, and two system-based design methods, Advanced Inelastic Analysis Method and Direct Design Method. A series of benchmark structural steel frames were first designed using a structural design optimization framework. System reliability analyses that included uncertainties in geometric properties, material properties, and applied loads were then performed on the resulting designs using the Importance Sampling technique. The findings indicate that component-based design methods consistently produce system-level reliabilities that exceed expected target levels; however, these design methods result in designs that are significantly heavier than those produced by system-based design methods. In contrast, the system-based design methods result in significantly lighter designs, with more consistent levels of reliability that are closer to expected target levels. Based on these findings, recommendations are provided to improve system-level reliability calibration procedures and to support the implementation of system-based design methods in future design codes.

29 **Keywords:** reliability-based design, structural design optimization, system reliability analysis, structural analysis,
30 structural systems, uncertainty quantification.

31 **1 INTRODUCTION**

32 For structural engineers, achieving designs that are materially efficient, as well as reliable, is paramount. The ability
33 to achieve such designs depends on the design methods that are available to engineers and their ability to account for
34 geometric and material nonlinearities, while ensuring adequate reliability. In terms of reliability – the focus of this
35 study – we distinguish two categories of design methods: (1) *component-based design methods*, which ensure
36 reliability at the level of individual components of a structural system and deem system failure to occur when the first
37 component fails, and (2) *system-based design methods*, which ensure reliability at the level of the entire structural
38 system and deem system failure to occur when the system’s strength is insufficient to resist the applied loads. Although
39 failure can be defined in many other ways related to serviceability, such as the event in which the peak roof or interstory
40 drift is reached or the maximum rotation capacity is attained, in this study we consider only strength-related limit
41 states. In this study, we investigate two component-based design methods that are implemented in the American
42 Institute of Steel Construction (AISC) 360-22 Specification for Structural Steel Buildings [1], the Direct Analysis
43 Method and the Advanced Elastic Analysis Method, and two system-based design methods, the Advanced Inelastic
44 Analysis Method implemented in the AISC 360-22 Specification, and the Direct Design Method being implemented
45 in the next cycle of the Australian and New Zealand design specifications. Detailed descriptions and motivation for
46 the development and implementation of each design method are given in the following sections.

47 **1.1 HISTORICAL DEVELOPMENT AND MOTIVATION**

48 The historical foundation for standardized design in the construction industry in the United States dates back to at
49 least 1923, when the Allowable Stress Design (ASD) framework was introduced in the 1st edition of the AISC
50 Specification [2]. Until 2005, the ASD framework was based on the principle that stresses developed in a structural
51 member due to nominal service loads must not exceed a certain fraction of the elastic limit, as determined by a safety
52 factor. The ASD framework attempted to ensure reliability by assigning a sufficiently high factor of safety against
53 failure, thereby addressing uncertainties in geometric properties, material properties, and applied loads implicitly.
54 Although structural steels, including those used in late 19th-century construction, exhibited substantial ductility, early
55 design practice did not include analytical tools or design philosophies capable of explicitly utilizing inelastic strength
56 reserves. As the understanding of structural behavior advanced, plastic design methods emerged, providing upper-

57 bound strength predictions that were significantly higher than elastic estimates and enabling engineers to rationally
58 exploit inelastic strength reserves. However, structural members continued to be designed within the same ASD
59 framework, which could not accommodate these types of material behavior and, as a result, often led to overly
60 conservative and materially inefficient designs.

61 The lack of a formal approach to account for inelastic material behavior and explicitly ensure reliability within the
62 ASD framework provided the incentive for the development of the Load and Resistance Factor Design (LRFD)
63 framework in the late 1970s and early 1980s [3,4]. In contrast to the ASD framework, the LRFD framework is based
64 on the ultimate strength of materials, which allows for utilization of both the elastic and plastic stages, and generally
65 leads to more materially efficient designs. More importantly, unlike the ASD framework, in which safety factors were
66 based on engineering judgment to account for uncertainties, the LRFD framework explicitly incorporates uncertainties
67 in geometric properties, material properties, and applied loads, allowing resistance and load factors to be determined
68 statistically by ensuring that target levels of reliability are consistently achieved.

69 In effect, the introduction of the LRFD framework within any design method – which dictates how structural analysis
70 must be carried out – enables assurance that target levels of reliability are consistently achieved. In component-based
71 design methods, which are typically based on variations of 1st- or 2nd-order elastic (geometrically nonlinear and
72 materially linear) structural analyses and largely govern the current design practice for structural steel buildings, the
73 LRFD framework is applied to individual structural members and connections to ensure reliability at the level of
74 individual components within a structural system. However, with recent advances and the increasing accessibility of
75 structural modeling and analysis tools, combined with the development of affordable desktop computers with the
76 processing and memory capacity required to complete advanced analyses at an acceptable runtime, there has been
77 growing interest in developing and adopting system-based design methods. In these design methods, which are based
78 on variations of 2nd-order inelastic structural analyses, the LRFD framework is applied to the entire structure to ensure
79 reliability at the system level. This is made possible because the use of 2nd-order inelastic (geometrically and materially
80 nonlinear) structural analyses explicitly accounts for most, if not all, component-level limit states directly in the
81 analysis, simplifying or eliminating separate component-level limit state checks while ensuring overall strength and
82 stability of the structure and accounting for beneficial inelastic load redistribution effects.

83 Despite the promising advantages of system-based design methods in achieving materially efficient designs of steel
84 structures [5,6], their widespread adoption has been hindered by limited guidance on calibration of system-level

85 resistance factors and insufficient data on the actual system-level reliabilities achieved in practice. Several studies
86 have attempted to address this gap: Buonopane and Schafer [7] evaluated the system-level reliabilities of structural
87 steel frames designed using 2nd-order inelastic analysis and proposed resistance factors based on plastic collapse
88 criteria, Shayan [8] developed a system reliability analysis framework for determining system-level resistance factors
89 for low- to mid-rise moment-resisting structural steel frames, demonstrating that system-based design methods can
90 provide uniform system-level reliabilities across various system-level failure modes, Zhang et al. [9,10] introduced
91 the Direct Design Method and conducted calibration studies for planar gravity-loaded structural steel frames based on
92 simplified system reliability analysis procedures. More recently, studies have extended system-based reliability
93 calibrations to stainless steel frames and spatial structures under combined loading conditions [11,12]. Despite these
94 advances, concerns remain as to whether system-based design methods can consistently meet target levels of reliability
95 across a broad range of structural configurations and loading scenarios in practice. For this reason, this study develops
96 a comprehensive framework for evaluating system-level reliability of a wide range of structural steel frames designed
97 using both component- and system-based methods. By comparing the Direct Analysis Method, Advanced Elastic
98 Analysis Method, Advanced Inelastic Analysis Method, and Direct Design Method across a range of benchmark
99 structural steel frames, this research aims to quantify the system-level reliability indices achieved by these design
100 methods, highlight design methods requiring recalibration, and provide recommendations toward broader adoption of
101 system-based design methods in future design codes for structural steel buildings.

102 **1.1.1 DESIGN CRITERION FOR COMPONENT-BASED DESIGN METHODS**

103 If we denote a structural analysis that incorporates all of the requirements of a specific component-based design
104 method and converts applied loads to actions on the structural members by $f(\cdot)$, then the design criterion for a
105 structural member in a structural system designed using the LRFD framework is given by the following inequality:

$$\phi_c R_{nc} \geq f\left(\sum_i \gamma_i q_{n,i}\right), \quad (1)$$

106 where ϕ_c is the component-level resistance factor corresponding to a limit state governing the response of the
107 structural member, R_{nc} is the nominal strength of the structural member against this limit state, $R_{rc} = f(\sum_i \gamma_i q_{n,i})$ is
108 the required strength of the structural member determined from the structural analysis, γ_i represent load factors from
109 the design load combinations that are considered during the design of the structure, and $q_{n,i}$ represent nominal loads
110 acting on the structure. Given that the strength checks, given by Eq. (1), are performed on the level of individual
111 structural components, with component-level resistance factor ϕ_c calibrated to ensure that a target level of component

112 reliability is always achieved, the specific design method is said to be categorized as a component-based design
113 method.

114 **1.1.2 DIRECT ANALYSIS METHOD**

115 In the 6th edition of the AISC Manual of Steel Construction [13], two significant improvements were introduced to the
116 AISC's long-standing approach based on the ASD framework: the concept of effective length and implicit
117 consideration of the 2nd-order effects. The concept of effective length was introduced to account for the influence of
118 the stiffness of a structural system on the strength of individual structural members subjected to compression. More
119 specifically, the allowable axial stress was determined using a column strength equation in which an effective length
120 KL replaced the actual unbraced length L . The effective length was obtained from an elastic buckling analysis or,
121 under a prescribed set of assumptions, could be evaluated using alignment charts. For structural members subjected
122 to combined compressive and flexural loads, bending stresses were computed using a 1st-order elastic analysis and
123 subsequently amplified to account for 2nd-order effects through a moment amplification factor incorporated directly
124 into the interaction equations. The compressive stresses appearing in this amplification factor were likewise evaluated
125 using the effective length, thereby maintaining consistency between the treatment of destabilizing effects of
126 compressive and flexural loads.

127 In the 1st edition of the AISC LRFD Specification for Structural Steel Buildings [14], the design approach shifted from
128 the implicit treatment of the 2nd-order effects – previously addressed through a moment amplification factor embedded
129 within the interaction equations – to an explicit and systematic consideration of structural stability. A dedicated chapter
130 on stability was introduced, which clearly stated that “*second-order (P-Δ) effects shall be considered in the design of*
131 *frames.*” Despite this shift, the structural members subjected to compressive loads continued to be designed using the
132 concept of effective length. For structural members subjected to combined compressive and flexural loads, the required
133 flexural strength in the interaction equations was now to be determined from a 2nd-order elastic analysis. As an
134 alternative to a 2nd-order elastic analysis, a moment amplification procedure – conceptually similar but more robust
135 than that used in the 6th edition of the AISC Manual of Steel Construction – was still permitted. In this procedure, the
136 compressive stresses governing the moment amplification factor continued to be computed using effective lengths,
137 thereby retaining the concept of effective length within the design practice.

138 A significant shortcoming of the heavy reliance on the concept of effective length within the stability provisions is the
139 difficulty of accurately determining effective lengths for structural members within structural system with complex

140 geometries. For this reason, in the early 2000s, the AISC formed a joint task committee together with the Structural
141 Stability Research Council to develop improved provisions for the design of steel structures that could better account
142 for geometric and material nonlinearities, while simplifying the design process by eliminating the need for the use of
143 effective length. Through a series of studies [15–21], the joint task committee developed the Direct Analysis Method
144 (DAM), which was formally introduced in the 2005 edition of the AISC 360 Specification [22] and remains largely
145 unchanged in its 2022 edition [1].

146 The key advantage of the DAM is that it eliminates the need to compute effective lengths KL . Instead, the DAM uses
147 the unbraced length L of a structural member when determining its nominal compressive strengths P_{nc} . However, in
148 exchange for this simplification, the DAM, which is based on 2nd-order elastic analysis (or geometrically nonlinear
149 analysis with initial system imperfections (GNIA) in European notation), requires (1) to apply a stiffness reduction to
150 the structural members and connections that provide lateral stability to the structural system to account for the effect
151 of yielding, which is often accentuated by the presence of residual stresses, and (2) to account for the initial system
152 imperfections directly in the analysis. The stiffness reduction has two components: (1) a general reduction factor of
153 0.80 is applied to all cross-sectional stiffnesses, and (2) for heavily compressed members, an additional stiffness
154 reduction factor τ_b is applied to the flexural stiffness EI . Taken together within the design process, the DAM requires
155 a reduction factor of 0.80 to the axial cross-sectional stiffnesses, such that $EA_g \rightarrow 0.80EA_g$, and a reduction factor of
156 $0.80\tau_b$ to the flexural cross-sectional stiffnesses, such that $EI \rightarrow 0.80\tau_b EI$. The initial system imperfections must be
157 included in the analysis either through explicit modeling or, alternatively, using equivalent notional loads.

158 With reference to Eq. (1), if we denote a structural analysis that incorporates all the requirements of the DAM by
159 $f_{\text{DAM}}(\cdot)$, then the design criterion for a structural member in a structure is given by the following inequality:

$$\phi_c R_{nc} \geq f_{\text{DAM}} \left(\sum_i \gamma_i q_{n,i} \right). \quad (2)$$

160 Given that the DAM's strength checks in Eq. (2) are performed on the level of each individual structural component
161 of a structural system, the DAM is categorized as a component-based design method.

162 **1.1.3 ADVANCED ELASTIC ANALYSIS METHOD**

163 The DAM relies on defining the unbraced lengths L of structural members subjected to compression, which in some
164 cases might be difficult, if not impossible, to do. As noted by Wang and Ziemian [23,24], examples of structures where
165 this problem arises include, but are not limited to, arches, tree columns, and Vierendeel trusses. Following a series of
166 studies [23–26], a new design method that extends the DAM was developed and introduced in the 2016 edition of the

167 AISC 360 Specification [27], termed here the Advanced Elastic Analysis Method (AEAM). This design method
 168 addresses conditions in which challenges exist in establishing the unbraced lengths L of structural members. Although
 169 the AEAM is similar to the DAM in almost all aspects, the key difference and advantage of the AEAM is that the
 170 nominal compressive strength P_{nc} of a structural member can be determined directly from its cross-sectional
 171 compressive strength, such that $P_{nc} = F_y A_g$, effectively allowing the unbraced lengths L to be taken as zero. To apply
 172 this design method, in addition to the initial system imperfections, an engineer is required to include initial member
 173 imperfections by direct modeling in a 2nd-order elastic analysis (or geometrically nonlinear analysis with initial
 174 member and system imperfections (GNIA) in European notation). By directly modeling initial member imperfections,
 175 the structural analysis captures 2nd-order P - δ effects explicitly, so that the internal moments and stability behavior of
 176 the member are represented directly in the analysis, and member capacity can be evaluated using beam-column
 177 interaction equations rather than column strength equations based on effective length. Because of this requirement to
 178 explicitly model member imperfections, this approach is sometimes also referred to as Direct Modeling of Member
 179 Imperfections or DMML.

180 With reference to Eq. (1), if we denote a structural analysis that incorporates all the requirements of the AEAM by
 181 $f_{\text{AEAM}}(\cdot)$, then the design criterion for a structural member in a structure is given by the inequality of the same form
 182 as the one for the DAM shown in Eq. (2):

$$\phi_c R_{nc} \geq f_{\text{AEAM}} \left(\sum_i \gamma_i q_{n,i} \right). \quad (3)$$

183 The only difference between the design criteria given by Eq. (2) and (3) is that the AEAM, unlike the DAM, requires
 184 the initial member imperfections to be directly modeled in the analysis. Otherwise, the AEAM falls within the same
 185 category of component-based design methods as the DAM, given that the AEAM's strength checks per Eq. (3), are
 186 also performed on the level of individual components.

187 **1.1.4 ADVANCED INELASTIC ANALYSIS METHOD**

188 Due to advances in and the increasing accessibility of nonlinear structural modeling and analysis tools over the past
 189 several decades, combined with the development of affordable desktop computers with the processing and memory
 190 capacity required to complete advanced analyses at an acceptable runtime, there has been a growing interest in
 191 developing and adopting design methods that are based on variations of 2nd-order inelastic analysis. Such design
 192 methods can explicitly account for (1) both geometric and material nonlinearities, (2) initial geometric (at both member
 193 and system levels) and material (residual stresses) imperfections, and (3) complex but beneficial inelastic load

194 redistribution interactions that occurs between structural members as a structural system approaches its strength limit
 195 state. Additionally, design methods based on the 2nd-order inelastic analysis can account for most, if not all, limit states
 196 of individual structural members of a structure, thereby simplifying or eliminating separate component-level strength
 197 checks while ensuring overall stability of a structural system. As a result, the 2010 edition of the AISC 360
 198 Specification [28] introduced a new design method, termed here the Advanced Inelastic Analysis Method (AIAM),
 199 which allowed an engineer to design steel structures using 2nd-order inelastic analysis and directly account for the
 200 geometric and material imperfections (or geometrically and materially nonlinear analysis with initial geometric
 201 (member and system) and material (residual stresses) imperfections (GMNIA) in European notation). It is also worth
 202 noting that this design method was not limited to fully restrained (rigid) moment connections, thereby superseding
 203 earlier design methods based on the plastic hinge analysis [29].

204 If we denote the structural analysis that incorporates all the requirements of the AIAM by $f_{AIAM}(\cdot)$, then the design
 205 criterion for an entire structure is given by the following inequality:

$$R_{ns}^* \geq f_{AIAM} \left(\sum_i \gamma_i q_{n,i} \right), \quad (4)$$

206 where R_{ns}^* is the reduced ultimate strength of the structure and $R_{rs} = f_{AIAM}(\sum_i \gamma_i q_{n,i})$ is the required strength of the
 207 structure determined from the analysis. In conducting the 2nd-order inelastic analyses, in which the applied loads are
 208 increased incrementally by using a load proportionality factor λ , the reduced ultimate strength of the entire structure
 209 can alternatively be denoted using $\lambda_{un}^* = R_{ns}^*/R_{rs}$ and the design criterion in Eq. (4) can be rewritten into a more
 210 convenient form:

$$\lambda_{un}^* \geq 1. \quad (5)$$

211 As can be observed from Eq. (5), no reductions are applied directly to the ultimate strength λ_{un}^* . Instead, in attempt to
 212 account for uncertainties and achieve an acceptable level of system reliability when using the AIAM, the AISC 360-
 213 22 Specification requires a reduction factor of 0.90 to be applied to the material properties – elastic modulus E and
 214 yield stress F_y – of structural members when performing the analysis. Thus, the ultimate strength λ_{un}^* obtained during
 215 the design process according to the AIAM is not the actual strength of a structure but is reduced due to the reduction
 216 factor of 0.90 already embedded in the structural analysis. However, as noted in the Commentary to Appendix 1 of
 217 the AISC 360-22 Specification, this reduction factor is assumed to be conservative, and no system reliability analyses
 218 were performed to calibrate it. The AIAM can be categorized as a system-based design method because it performs a
 219 strength check, given by Eq. (5), on the level of the entire structural system. However, it remains uncalibrated and,

220 thus, does not guarantee that any particular level of target reliability is always achieved, further highlighting the need
221 for the present study.

222 **1.1.5 DIRECT DESIGN METHOD**

223 To address the limitations of the AIAM – namely, its inability to ensure that a target level of system reliability is always
224 achieved – Zhang et al. [9,10] proposed a new design method based on 2nd-order inelastic analysis (or geometrically
225 and materially nonlinear analysis with initial geometric (member and system) and material (residual stresses)
226 imperfections (GMNIA) in European notation), termed the Direct Design Method (DDM), which, unlike the AIAM,
227 does not require an engineer to apply any reductions during the analysis process, thus simplifying the design process
228 by allowing an engineer to model a structure "as is." To ensure that an acceptable level of system reliability is achieved,
229 the DDM employs a system-level resistance factor ϕ_s that is applied to the nominal ultimate strength of a structure,
230 such that the design criterion is given by

$$\phi_s R_{ns} \geq f_{\text{DDM}} \left(\sum_i \gamma_i q_{n,i} \right), \quad (6)$$

231 which, alternatively, can be rewritten as

$$\phi_s \lambda_{un} \geq 1. \quad (7)$$

232 In the DDM, any target level of reliability can be, in principle, achieved by calibrating ϕ_s in Eq. (7) through rigorous
233 system reliability analysis. Such analysis was performed by Zhang et al. [9,10], that recommended using ϕ_s of 0.85
234 for low- and mid-rise structural steel frames, a value which is used in this study, based on nominal loads and load
235 factors obtained from the ASCE 7-22 Standard [30]. This calibration corresponds to a system-level reliability index β
236 of 2.9 for structural steel frames subjected to gravity loads only and 2.7 for structural steel frames subjected to
237 combined gravity and wind loads. When using the nominal loads and load factors specified in the AS/NZS 1170
238 Standard [31,32] ϕ_s of 0.90 is obtained for the gravity loads only combination, corresponding to system-level
239 reliability indices β of 3.0 and 3.2 for planar and spatial steel frames, respectively. The ϕ_s of 0.90 is used in the draft
240 revised Australian standard for steel structures AS 4100 [33] and is the same system resistance factor as that previously
241 implemented in the Australian and New Zealand design standards for cold-formed steel structures AS/NZS 4600 [34],
242 steel storage racks AS 4084.1 [35] and formwork structures AS 3610.2 [36]. For this reason, in addition to studying
243 the system-level reliabilities achieved by the DDM with $\phi_s = 0.85$ ($\lambda_{un} \geq 1.18$), the system-level reliabilities
244 achieved by the DDM with $\phi_s = 0.90$ ($\lambda_{un} \geq 1.11$) are also studied herein. To distinguish between these two
245 implementations, the DDM with $\phi_s = 0.85$ and $\phi_s = 0.90$ are referred to as DDM85 and DDM90, respectively.

246 **1.2 GENERAL PROCEDURE**

247 To investigate the system-level reliabilities achieved by the considered design methods, a series of benchmark
248 structural steel frames were first designed using a structural design optimization framework and analyzed using 2nd-
249 order inelastic analysis. System reliability analyses that included uncertainties in geometric properties, material
250 properties, and applied loads were then performed on the ultimate strengths of the resulting optimal designs using the
251 Importance Sampling technique. This general procedure enabled consistent comparison between the system-level
252 reliabilities achieved by the design methods of interest.

253 **2 DESIGN PROCESS**

254 **2.1 STRUCTURAL STEEL FRAMES OF INTEREST**

255 To investigate the system reliabilities achieved by the considered design methods, the structural steel frames presented
256 by Ziemian and Ziemian [37] are selected for comparison. These structural steel frames, presented in Fig. 1, represent
257 a wide range of geometric configurations, showcasing varying sensitivities to geometric and material nonlinearities.
258 In all frames, the structural members are oriented to experience flexure about their major axes, except for structural
259 steel frames #8 and #10 in which the columns are oriented to experience flexure about their minor axes. The structural
260 steel frames are also assumed to be fully braced out-of-plane, allowing for fully planar analyses and precluding spatial
261 effects. This approach is justified by system reliability studies which demonstrated that planar and spatial frames have
262 nearly identical system-level reliability indices when designed by the DDM [38,39]. While the load magnitudes
263 provided in [37] are retained for further design according to the design methods considered in this study, the elastic
264 moduli E and yield stresses F_y for all frames are assumed to be 200 GPa (29,000 ksi) and 345 MPa (50 ksi),
265 respectively. The magnitudes of the loads applied to the benchmark structural steel frames can be found in the
266 Supplementary Materials.

267 **2.2 DESIGN LOADS AND LOAD COMBINATIONS**

268 Instead of considering only one load combination per structural steel frame during the design process, as was done in
269 [37], we consider the following set of load combinations from the American Society of Civil Engineers (ASCE)
270 Standard for Minimum Design Loads and Associated Criteria for Buildings and Other Structures [30], with their
271 references in the Standard provided, given that the benchmark structural steel frames, collectively, are subjected to
272 various combinations of dead D_n , floor live L_{fn} , roof live L_{rn} , and wind W_n loads:

$$\left\{ \begin{array}{l} 1a: 1.4D_n \\ 2a: 1.2D_n + 1.6L_{fn} + 0.5L_{rn} \\ 3a.1: 1.2D_n + 0.5L_{fn} + 1.6L_{rn} \\ 3a.2: 1.2D_n + 1.6L_{rn} + 0.5W_n \\ 4a: 1.2D_n + 0.5L_{fn} + 0.5L_{rn} + 1.0W_n \\ 5a: 0.9D_n + 1.0W_n \end{array} \right. , \quad (8)$$

273 For the work reported here, we assume that roof live loads L_{rn} and floor live loads L_{fn} are statistically identical, and
 274 no distinction is made between the two. Accordingly, the load factors for floor live loads γ_{L_f} are used in place of those
 275 for roof live loads γ_{L_r} . This assumption has been adopted in several previous studies investigating system reliabilities
 276 achieved by various design methods [9,10,39–41] and provides an important frame of reference for comparative
 277 evaluation. Recent studies that have focused on providing statistically supported load models for roof live loads L_{fn}
 278 [42,43] suggest that this assumption may be overly conservative. However, the explicit incorporation of these recent
 279 roof load models is beyond the scope of the present study and is therefore not pursued here. The authors intend to
 280 revisit this assumption in future work as improved data become available. Under this assumption, the set of considered
 281 load combinations in Eq. (8) can be rewritten as

$$\left\{ \begin{array}{l} 1a: 1.4D_n \\ 2a: 1.2D_n + 1.6L_{fn} + 1.6L_{rn} \\ 3a.1: 1.2D_n + 0.5L_{fn} + 0.5L_{rn} \\ 3a.2: 1.2D_n + 0.5W_n \\ 4a: 1.2D_n + 0.5L_{fn} + 0.5L_{rn} + 1.0W_n \\ 5a: 0.9D_n + 1.0W_n \end{array} \right. , \quad (9)$$

282 Observing that load combination 4a always controls over load combinations 3a.1, 3a.2, and 5a, the set of considered
 283 load combinations in Eq. (9) finally simplifies to

$$\left\{ \begin{array}{l} 1a: 1.4D_n \\ 2a: 1.2D_n + 1.6L_{fn} + 1.6L_{rn} \\ 4a: 1.2D_n + 0.5L_{fn} + 0.5L_{rn} + 1.0W_n \end{array} \right. , \quad (10)$$

284 which is used during the design of all 22 structural steel frames according to all considered design methods.

285 Current design codes do not explicitly stipulate whether proportional or nonproportional loading should be used during
 286 the design process when lateral loads are present. Therefore, this study considers both approaches to provide engineers
 287 with additional insight into how the choice of load proportionality affects the design process and the resulting system-
 288 level reliabilities.

289 **2.3 SECTION SELECTION**

290 The structural analyses used to design the structural steel frames were performed using line finite elements, which are
 291 incapable of capturing member limit states associated with cross-sectional instabilities, such as local buckling. For
 292 this reason, the selection of sections was restricted to W-shaped sections listed in the 16th edition of the AISC Steel
 293 Construction Manual [44] that are classified as both compact in flexure about both major and minor axes and

294 nonslender in axial compression, as specified by the requirements of Chapter B of the AISC 360-22 Specification.
 295 This restriction ensures that the sections used in the final designs of the structural steel frames can reach their plastic
 296 capacity and generally develop a normalized rotation capacity of 3 before cross-sectional instabilities occur, thereby
 297 justifying the use of line finite elements in the conducted structural analyses. Out of the 289 W-shaped sections listed
 298 in the AISC Steel Construction Manual, 168 were found to be compact in flexure about both the major and minor axes
 299 and nonslender in axial compression. Additionally, following standard practice, the selection of sections for columns
 300 was further restricted to W8X... through W14X... sections. As a result, during the design of the structural steel frames
 301 according to the considered design method, 168 sections were available for the selection of beams and braces, and 72
 302 sections were available for the selection of columns.

303 **2.4 DESIGN CRITERIA AND LIMIT STATES**

304 In this study, the scope of the design is restricted to limit states of structural members only and connection limit states
 305 are not considered. Instead, beam-to-column connections are idealized as either perfectly pinned or fully rigid,
 306 consistent with common practice in prior system reliability studies of structural steel frames. This modeling choice is
 307 intended to isolate and examine the baseline structural response of the structural steel frames without the added
 308 complexity associated with connection behavior. Recent work has begun to explore the role of partially restrained
 309 connections within the context of the DDM [45–47]. Incorporating such effects into system reliability-based design
 310 remains an important topic for future research but is beyond the scope of the present study.

311 For component-based design methods – DAM and AEAM – we consider three possible limit states for each structural
 312 member:

- 313 1. If a structural member is subjected to pure tensile load, such that $P_r > 0$ and $M_r = 0$, the design criteria in
 314 Eq. (2) and (3) can be rewritten as

$$\phi_{ct} P_{nt} \geq |P_r|, \quad (11)$$

315 where ϕ_{ct} is the component-level resistance factor related to the tensile yielding in the gross cross-section of
 316 the structural member and is equal to 0.90, and P_{nt} is the nominal tensile strength of the structural member
 317 determined in accordance with Chapter D of the AISC 360-22 Specification.

- 318 2. If a structural member is subjected to pure compressive load, such that $P_r < 0$ and $M_r = 0$, the design criteria
 319 in Eq. (2) and (3) can be rewritten as

$$\phi_{cc} P_{nc} \geq |P_r|, \quad (12)$$

320 where ϕ_{cc} is the component-level resistance factor related to the compressive buckling of the structural
 321 member and is equal to 0.90, and P_{nc} is the nominal compressive strength of the structural member
 322 determined in accordance with Chapter E of the Specification. For the DAM, P_{nc} is computed with $K = 1$
 323 and, for the AEAM, P_{nc} is computed as $F_y A_g$.

324 3. If a structural member is subjected to combined axial and flexural load, such that $|P_r| \geq 0$ and $M_r \neq 0$, the
 325 design criteria in Eq. (2) and (3) can be rewritten as

$$\begin{cases} \frac{|P_r|}{P_c} + \frac{8|M_r|}{9M_c} \leq 1, & \frac{|P_r|}{P_c} \geq 0.2 \\ \frac{1}{2} \frac{|P_r|}{P_c} + \frac{|M_r|}{M_c} \leq 1, & \frac{|P_r|}{P_c} < 0.2 \end{cases}, \quad (13)$$

326 where P_c is the available axial design strength, either tensile or compressive depending on whether the
 327 structural member is experiencing pure tension or compression, and $M_c = \phi_{cb} M_n$ is the available flexural
 328 design strength with ϕ_{cb} being the component-level resistance factor related to the yielding due to flexure
 329 and is equal to 0.90, and M_n is the nominal flexural strength determined in accordance with Chapter F of the
 330 AISC 360-22 Specification. In all cases, members are assumed as fully braced out-of-plane resulting in the
 331 nominal flexural strength taken as $M_n = M_p$.

332 Combined, the limit states given by Eq. (11), (12), and (13) constitute the design criteria, denoted by s_i^j , which must
 333 be satisfied for each structural member i for each load combination j considered during the design process, given by

$$s_i^j = \begin{cases} |P_{r,i}^j| - \phi_{ct} P_{nt,i} \leq 0, & P_{r,i}^j > 0 \text{ and } M_{r,i}^j = 0 \\ |P_{r,i}^j| - \phi_{cc} P_{nc,i} \leq 0, & P_{r,i}^j < 0 \text{ and } M_{r,i}^j = 0 \\ \frac{|P_{r,i}^j|}{P_{c,i}} + \frac{8|M_{r,i}^j|}{9M_{c,i}} - 1 \leq 0, & \frac{|P_{r,i}^j|}{P_{c,i}} \geq 0.2 \text{ and } |M_{r,i}^j| \neq 0 \\ \frac{1}{2} \frac{|P_{r,i}^j|}{P_{c,i}} + \frac{|M_{r,i}^j|}{M_{c,i}} - 1 \leq 0, & \frac{|P_{r,i}^j|}{P_{c,i}} < 0.2 \text{ and } |M_{r,i}^j| \neq 0 \end{cases} \quad (14)$$

334 where the required strength P_r and M_r are determined from the 2nd-order elastic analysis.

335 Similarly, for the system-based design methods – AIAM and DDM – the design criteria, denoted by s^j , are simply
 336 given by Eq. (5) for the AIAM and Eq. (7) for the DDM. These design criteria are checked for each load combination
 337 j considered during the design process. For the AIAM, the design criterion is given by

$$s^j = 1 - \lambda_{un}^* \leq 0, \quad (15)$$

338 and, for the DDM, the design criterion is given by

$$s^j = 1 - \phi_s \lambda_{un}^j \leq 0, \quad (16)$$

339 where the ultimate strengths λ_{un}^* (AIAM) and λ_{un}^j (DDM) are determined from the 2nd-order inelastic analysis.

2.5 STRUCTURAL DESIGN OPTIMIZATION

For a robust investigation of the system-level reliabilities achieved by the considered design methods, it is important to obtain the most optimal designs of the benchmark structural steel frames, with least possible weight, that satisfy all the requirements of each considered design method. In doing so, we attempt to ensure that a minimum level of system reliability will be explored for each design method and structural steel frame of interest. Although a more comprehensive objective function could incorporate fabrication, erection, inspection, and life-cycle maintenance costs, minimizing such costs would result in designs with higher strength and, thus, higher reliability than those obtained by minimizing for the weight alone, and would therefore not expose the lower bounds of system-level reliability that are central to this study. While it is possible to achieve optimal least-weight designs manually through a trial-and-error approach for simple structural steel frames with only a few structural members, this approach quickly becomes impractical for more complex structural steel frames with many structural members. To address this challenge, we have developed and employed a structural design optimization framework to systematically identify the designs with least possible weight that meet all the requirements of each considered design method, which serve as constraints in the structural design optimization problem at hand.

In general, the process of structural design can be formulated as a well-posed mathematical optimization problem, where the weight $W = W(\vec{p})$ of a structure must be minimized with respect to the parameters \vec{p} that describe the structure and serve as the design variables. In the case of this study, the parameters \vec{p} are the cross-sectional dimensions and properties of the W-shaped sections available for selection during the design of the benchmark structural steel frames and, thus, the structural design optimization problem at hand is discrete in nature. For this reason, it is convenient to introduce a new set of N_{SM} integer design variables $\vec{\alpha}$, where N_{SM} is the number of structural members in a structural steel frame of interest, with respect to which the optimization will be performed, such that $\vec{p} = \vec{p}(\vec{\alpha})$ and $W = W(\vec{\alpha})$. In effect, the i^{th} component of the design vector $\vec{\alpha}$ defines the W-shaped section that will be prescribed to the i^{th} structural member of a structural steel frame from the list of sections available for selection.

2.5.1 CONSTRAINTS

2.5.1.1 STRENGTH CONSTRAINTS

As mentioned earlier, the structural design optimization should not only result in optimal designs, with least possible weight, but also satisfy the requirements – *strength constraints* – imposed by each design method and given by the design criteria in Eq. (14), (15), and (16).

368 **2.5.1.2 CONSTRUCTABILITY CONSTRAINTS**

369 In this study, serviceability limit states are not imposed as an additional set of constraints in the structural design
 370 optimization framework, as they typically dominate the design process by imposing, albeit implicitly, much stricter
 371 constraints on the overall stiffness of a structure than the strength constraints. However, we do incorporate
 372 *constructability constraints* to ensure geometric compatibility between the structural members at the connection
 373 locations, which are typically omitted in the previous studies on the structural design optimization. In this study, the
 374 three types of constructability constraints shown in Fig. 2 are considered:

- 375 1. At the beam-to-column connections, if the column is oriented to bend about its major axis, the flange width
 376 of the column $b_{f,c}$ must be greater than or equal to the flange width of the beam $b_{f,b}$.
- 377 2. At the beam-to-column connections, if the column is oriented to bend about its minor axis, the web depth of
 378 the column $d_c - 2t_{f,c}$ must be greater than or equal to the flange width of the beam $b_{f,b}$.
- 379 3. At the column-to-column connections, both the depth d_{bc} and flange width $b_{f,bc}$ of the bottom column must
 380 be greater than or equal to the depth d_{tc} and flange width $b_{f,tc}$ of the top column.

381 If there are N_{BCC} beam-to-column connections in a structure, the constructability constraints at the k^{th} beam-to-column
 382 connection, denoted by $c_1^k = c_1^k(\vec{\alpha})$, can be expressed as

$$c_1^k = \begin{cases} b_{f,b} - b_{f,c} \leq 0, & \text{column bending about major axis} \\ b_{f,b} - (d_c - 2t_{f,c}) \leq 0, & \text{column bending about minor axis} \end{cases} \quad (17)$$

383 and, similarly, if there are N_{CCC} column-to-column connections in a structure, the constructability constraints at the ℓ^{th}
 384 column-to-column connection, denoted by $c_2^\ell = c_2^\ell(\vec{\alpha})$ and $c_3^\ell = c_3^\ell(\vec{\alpha})$, can be expressed as

$$c_2^\ell = d_{tc} - d_{bc} \leq 0, \quad (18)$$

$$c_3^\ell = b_{f,tc} - b_{f,bc} \leq 0. \quad (19)$$

385 **2.5.1.3 SYMMETRY CONSTRAINTS**

386 In addition to constructability constraints, following standard practice, we also impose *symmetry constraints*. These
 387 constraints allow us to assign the same section to different groups of structural members, thereby reducing the number
 388 of unique sections required for construction of a particular structural steel frame. For example, it is common to assign
 389 identical sections to the inner and outer beams of each floor, as well as to the inner and outer columns. While symmetry
 390 can, in principle, be enforced through explicit equality constraints of the form $\alpha_i = \alpha_j$ if two structural members i and
 391 j share the same section, such constraints are difficult to handle efficiently within the Genetic Algorithm used as the
 392 optimizer in the developed structural design optimization framework. To address this issue, we introduce a new set of
 393 N_{IDV} independent integer design variables $\vec{\omega}$, where $N_{IDV} \leq N_{SM}$ is the number of independent design variables $\vec{\omega}$,

394 with the original design variables $\vec{\alpha}$ becoming dependent on $\vec{\omega}$ via a predefined function $\vec{\alpha} = m(\vec{\omega})$ that maps the
395 independent to dependent design variables. The introduction of the independent design variables $\vec{\omega}$ allows us to mimic
396 the equality constraints and automatically satisfy them by ensuring that two structural members i and j share the same
397 section if they are assigned the same independent design variable ω_k , such that $\alpha_i = \alpha_j = \omega_k$. The introduction of the
398 independent design variables $\vec{\omega}$ provides two additional key benefits: (1) it reduces the dimensionality of the structural
399 design optimization problem by grouping structural members into categories governed by a single independent design
400 variable, and (2) it reduces the number of unique constructability constraints that must be satisfied for a given structural
401 steel frame by reducing the number of unique beam-to-column and column-to-column connections.

402 The mapping between the independent and dependent design variables for structural steel frames #1 to #11 with
403 irregular geometries can be found in the Supplementary Materials. The inner beams, outer beams, inner columns, and
404 outer columns are assumed to have the same section every two floors for structural steel frames #12 to #19, every
405 three floors for structural steel frames #20 and #21, and every four floors for frame #22.

406 2.5.2 GENETIC ALGORITHM

407 To summarize, the structural design optimization problem can be formulated mathematically as:

$$\begin{aligned}
&\text{minimize} && W = \rho \sum_{i=1}^{N_{SM}} L_i A_{g,i}(\vec{\omega}) \text{ with respect to } \vec{\omega}, \\
&\text{subject to} && \textit{Box constraints} \\
&&& \text{For beams and braces:} && 1 \leq \omega_i \leq 168, && i \in \{1, \dots, N_{IDV}\}, \\
&&& \text{For columns:} && 1 \leq \omega_i \leq 72, && \\
&&& \textit{Strength constraints} \\
&&& \text{For DAM:} && s_i^j(\vec{\omega}) \leq 0 \text{ in Eq. (14),} && i \in \{1, \dots, N_{SM}\}, \\
&&& \text{For AEAM:} && s_i^j(\vec{\omega}) \leq 0 \text{ in Eq. (14),} && j \in \{1, \dots, N_{DLC}\}, && (20) \\
&&& \text{For AIAM:} && s^j(\vec{\omega}) \leq 0 \text{ in Eq. (15),} && j \in \{1, \dots, N_{DLC}\}, \\
&&& \text{For DDM:} && s^j(\vec{\omega}) \leq 0 \text{ in Eq. (16),} && \\
&&& \textit{Constructability constraints} \\
&&& \text{For beam-to-column connections:} && c_1^k(\vec{\omega}) \leq 0 \text{ in Eq. (17),} && k \in \{1, \dots, N_{BCC}\}, \\
&&& \text{For column-to-column connections:} && c_2^\ell(\vec{\omega}) \leq 0 \text{ in Eq. (18),} && \ell \in \{1, \dots, N_{CCC}\}, \\
&&& && c_3^\ell(\vec{\omega}) \leq 0 \text{ in Eq. (19),} &&
\end{aligned}$$

408 where ρ is the density of structural steel assumed to be 8000 kg/m³ (0.290 lb/in.³), L_i is the length of the i^{th} structural
409 member, and N_{DLC} is the number of design load combinations considered during the design process and is equal to 3
410 in the present study.

411 The structural design optimization problem formulated in Eq. (20) was solved using the Genetic Algorithm (GA) [48]
412 implemented in the `Metaheuristics.jl` package [49], an open-source package written in the Julia programming
413 language that implements several global optimization metaheuristic algorithms for solving single- and multi-objective
414 optimization problems. A key distinction of the implementation of the GA in the `Metaheuristics.jl` package,

415 compared to other implementations that typically rely on the Penalty Method to guide the algorithm toward the
416 constrained optimum, is its use of the Constrained Violation Rule [50]. Unlike the Penalty Method, which penalizes
417 the objective function for constraint violations, the Constrained Violation Rule computes the average constraint
418 violation to perform pairwise comparisons of individuals in the population during the selection process; thus, enabling
419 the algorithm to focus on feasibility during the optimization process without relying on arbitrary penalty parameters.
420 Moreover, the Constrained Violation Rule ensures that the entire population will reach the feasible region if at least
421 one feasible solution is identified or provided.

422 In the used structural design optimization framework, the Binary Tournament Selection was used as the selection
423 operator to ensure that fitter individuals had a higher probability of being chosen while maintaining diversity within
424 the population, the Simulated Binary Crossover [51] was used as the crossover operator to generate offspring solutions
425 by combining the genetic material of parent solutions in a way that encourages exploration of the design space, and
426 the Polynomial Mutation [52] was used as the mutation operator to introduce small and controlled variations to
427 individual solutions, thus improving the algorithm's ability to escape local optima. Additionally, an elitist strategy was
428 used to ensure that the fittest individuals from the current generation were carried over to the next, thereby preserving
429 high-quality solutions throughout the structural design optimization process. Note that while many other options exist
430 for the selection, crossover, and mutation operators, the described setup had demonstrated the best convergence rates.

431 **2.5.3 FINITE ELEMENT MODELING AND ANALYSIS**

432 For the purposes of the structural design optimization, the 2nd-order elastic and inelastic analyses were performed
433 using OpenSeesPy, an open-source Python package for finite element analysis [53]. For designs according to the
434 component-based design methods, elastic beam-column finite elements based on Euler-Bernoulli beam theory were
435 used to model the structural members, and for designs according to the system-based design methods, which explicitly
436 consider material nonlinearities, displacement-based finite elements with fiber-type sections. The material assigned to
437 the structural members was modeled using elastic-perfectly plastic constitutive model. In all cases, each structural
438 member was discretized into four finite elements. For the 2nd-order inelastic analyses for the AIAM and DDM, similar
439 to the approach used in [9,10], the European Convention for Constructional Steelwork's self-equilibrating residual
440 stress pattern was adopted.

441 Following Ziemian and Ziemian [37], for structural steel frames with multiple lean-on columns, the lean-on columns
442 were modeled as a single column line on each side of the structural steel frame. The initial nominal frame out-of-

443 plumbness imperfections ψ_n with magnitude 1/500 were modeled directly in the directions indicated in Fig. 1 to avoid
444 the development of fictitious shear forces and moments during the analyses. For the AEAM, AIAM, and DDM, the
445 initial nominal member out-of-straightness imperfections δ_n of magnitude $L/1000$ were also modeled directly: to
446 induce the largest 2nd-order P - δ effects beams were assumed to have downward camber and columns were assumed
447 to have camber in the direction opposite to the applied wind loads (i.e., to the right for leftward wind loads and to the
448 left for rightward wind loads).

449 For proportional loading designs, gravity and wind loads were increased simultaneously while maintaining a constant
450 load ratio. For nonproportional loading designs, a sequential procedure was adopted: frames subjected to gravity loads
451 only were analyzed using a pushdown analysis in which the gravity loads were increased to failure, whereas frames
452 subjected to combined gravity and wind loads were analyzed using a pushover analysis in which the gravity loads
453 were applied first and the wind loads were then increased to failure.

454 To appropriately account for potentially large deflections during the exploration of the design space by the GA, the
455 corotational geometric transformation was used in the analyses according to all considered design methods. For the
456 DAM and AEAM, the Load Control Method was employed to incrementally apply the loads, while for the AIAM and
457 DDM, the Arclength Control Method was used.

458 **2.6 PROCEDURE**

459 For each benchmark structural steel frame, the structural design process according to a design method of interest was
460 performed using the following procedure:

- 461 1. A set of 1,000 initial candidate designs was created by generating 1,000 random independent design vectors
462 $\vec{\omega}$ to establish the initial population in the GA.
- 463 2. For each candidate design in a population, (1) its independent design variables $\vec{\omega}$ were mapped to dependent
464 design variables $\vec{\alpha}$, (2) cross-sectional dimensions and properties \vec{p} were extracted, (3) objective function
465 value W – weight – was computed, (4) strength constraint values \vec{S} were computed by performing either 2nd-
466 order elastic or inelastic analysis based on the design method of interest, (5) constructability constraint values
467 \vec{C} were computed, (6) average constraint violation values were computed, and (7) passed back to the GA.
- 468 3. Based on the values of the objective function and average constraint violation of all candidate designs in the
469 current generation, the GA generated the next generation of candidate designs by applying selection,
470 crossover, and mutation operators on the independent design vectors $\vec{\omega}$.

471 4. Steps 2 and 3 were repeated until the whole population converged to the final solution – optimal design of
472 the structural steel frame, with least possible weight, that meets all the requirements of the design method of
473 interest.

474 Note that the described procedure is general and can be applied to any design method, including those not considered
475 in the present study. The only step that is different is the computation of strength constraints, which differs between
476 the design methods. Additional flowcharts describing the step-by-step procedure of computing the strength constraints
477 – the most computationally intensive part of the structural design optimization – for each of the considered design
478 methods can be found in the Supplementary Materials. Results of the final optimal designs for the benchmark
479 structural steel frames designed according to the design methods of interest are provided in Section 4.

480 **3 SYSTEM RELIABILITY ANALYSIS**

481 **3.1 LIMIT STATE FUNCTION FORMULATION**

482 For the purposes of system reliability analysis, failure of a structure is defined as the event in which the structure
483 reaches its ultimate strength under a given random load combination. In the structural analyses performed in this study,
484 the ultimate strength of a structure is defined by the ultimate random load proportionality factor λ_u that the structure
485 can sustain before total loss of its load-carrying capacity, such that λ_u is less than unity. This definition of failure is
486 based on strength considerations only as no serviceability-related limit states, such as interstory drift or roof
487 displacement limits, are considered during the design process. Accordingly, the limit state function for a single random
488 load combination is given by

$$489 \quad g(\vec{X}) = \lambda_u(\vec{X}) - 1, \quad (21)$$

490 where λ_u is obtained from a 2nd-order inelastic analysis with random loads applied using nonproportional loading that
491 better represents the real-life loading conditions, and \vec{X} is the vector of N_{RV} random variables associated with
492 uncertainties in geometric properties, material properties, and applied loads that fully define the system reliability
493 problem for the structure.

494 If there are N_{RLC} random load combinations that must be considered for the structure, then the failure of the structure
495 is defined as an event in which the ultimate random strength is insufficient to resist the random loads associated with
496 any of the considered random loads, such that the limit state function is given by

$$497 \quad G(\vec{X}) = \min\{g_1(\vec{X}), \dots, g_{N_{RLC}}(\vec{X})\}, \quad (22)$$

496 which effectively represents a typical limit state function for series systems, where system failure occurs when any
 497 one of its failure modes is reached. In the case of this study, a failure mode of a system refers to the failure of a
 498 structure under one of the considered random load combinations.

499 3.2 RANDOM LOAD COMBINATIONS

500 The benchmark structural steel frames, collectively, are subjected to various combinations of dead D_n , floor live L_{fn} ,
 501 roof live L_{rn} , and wind W_n loads; therefore, the random demand $Q(\vec{x}, t)$ on a frame can be represented as a linear
 502 combination of random processes associated with dead $D(\vec{x}, t)$, floor live $L_f(\vec{x}, t)$, roof live $L_r(\vec{x}, t)$, and wind $W(\vec{x}, t)$
 503 loads, such that

$$Q(\vec{x}, t) = D(\vec{x}, t) + L_f(\vec{x}, t) + L_r(\vec{x}, t) + W(\vec{x}, t). \quad (23)$$

504 Estimating the statistics of these random processes is a challenging task given that they exhibit space and time
 505 dependence, except for the dead load $D(\vec{x}, t)$. For this reason, numerous load combination models were developed
 506 over the years to address this issue, among which Turkstra's Rule [54] is the simplest and most practical, and as such,
 507 serves as the foundation for the LRFD methods' load combinations [3,55]. Turkstra's Rule assumes that when a load
 508 reaches its maximum value in the design lifetime of a structure, other loads are most likely to be at their arbitrary
 509 point-in-time values. Applying Turkstra's Rule to Eq. (23) allows us to remove the dependence on space and time by
 510 converting the random processes into arbitrary point-in-time $(\cdot)_{apt}$ and lifetime maximum $(\cdot)_{max}$ random variables,
 511 resulting in the following set of the random load combinations:

$$\begin{cases} 1: D_{max} + L_{f,apt} + L_{r,apt} + W_{apt} \\ 2: D_{apt} + L_{f,max} + L_{r,apt} + W_{apt} \\ 3: D_{apt} + L_{f,apt} + L_{r,max} + W_{apt} \\ 4: D_{apt} + L_{f,apt} + L_{r,apt} + W_{max} \end{cases} \quad (24)$$

512 Due to the inherently low variability of the dead load, it is assumed that the arbitrary point-in-time dead load D_{apt} and
 513 lifetime maximum dead load D_{max} are the same, such that $D = D_{apt} = D_{max}$. For simplicity, it is also assumed that
 514 the contribution of the arbitrary point-in-time wind load W_{apt} is negligible given that its expected value is close to
 515 zero [3]. Applying these assumptions and factoring out the nominal load, the set of random load combinations in Eq.
 516 (24) simplifies to

$$\begin{cases} 1: X_D D_n + X_{L_f}^{apt} L_{fn} + X_{L_r}^{apt} L_{rn} \\ 2: X_D D_n + X_{L_f}^{max} L_{fn} + X_{L_r}^{apt} L_{rn} \\ 3: X_D D_n + X_{L_f}^{apt} L_{fn} + X_{L_r}^{max} L_{rn} \\ 4: X_D D_n + X_{L_f}^{apt} L_{fn} + X_{L_r}^{apt} L_{rn} + X_W^{max} W_n \end{cases}, \quad (25)$$

517 where $X_D = D/D_n$, $X_{L_f}^{apt} = L_{f,apt}/L_{fn}$, $X_{L_f}^{max} = L_{f,max}/L_{fn}$, $X_{L_r}^{apt} = L_{r,apt}/L_{rn}$, $X_{L_r}^{max} = L_{r,max}/L_{rn}$, and $X_W^{max} =$
518 W_{max}/W_n are the normalized random variables associated with the dead, arbitrary point-in-time floor live, lifetime
519 maximum floor live, arbitrary point-in-time roof live, lifetime maximum roof live, and lifetime maximum wind loads,
520 respectively.
521 As discussed earlier in the context of design load combinations and consistent with prior system reliability studies
522 [9,10,39–41], we assume that random roof live loads L_r are statistically equivalent to random floor live loads L_f , and
523 no distinction is made between the two. This assumption simplifies the formulation of the random load combinations
524 while remaining aligned with existing practice; the implications of this assumption will be examined in future work.
525 At the same time, the described probabilistic framework for formulation of the random load combinations is retained
526 to facilitate future studies. Under this assumption, the set of considered random load combinations in Eq. (25) can be
527 rewritten as

$$\begin{cases} 1: X_D D_n + X_{L_f}^{apt} L_{fn} + X_{L_r}^{apt} L_{rn} \\ 2: X_D D_n + X_{L_f}^{max} L_{fn} + X_{L_r}^{max} L_{rn} \\ 3: X_D D_n + X_{L_f}^{apt} L_{fn} + X_{L_r}^{apt} L_{rn} \\ 4: X_D D_n + X_{L_f}^{apt} L_{fn} + X_{L_r}^{apt} L_{rn} + X_W^{max} W_n \end{cases} \quad (26)$$

528 Observing that the random load combination 1 is the same as the random load combination 3, the set of considered
529 random load combinations can be simplified to

$$\begin{cases} 1: X_D D_n + X_{L_f}^{apt} L_{fn} + X_{L_r}^{apt} L_{rn} \\ 2: X_D D_n + X_{L_f}^{max} L_{fn} + X_{L_r}^{max} L_{rn} \\ 3: X_D D_n + X_{L_f}^{apt} L_{fn} + X_{L_r}^{apt} L_{rn} + X_W^{max} W_n \end{cases} \quad (27)$$

530 which was used to evaluate the system-level reliabilities of the optimal structural steel frame designs.

531 3.3 STATISTICS OF RANDOM VARIABLES

532 The statistics of the normalized random variables associated with loads are based on the statistics provided by
533 Akchurin et al. [56], which were assembled primarily from the early studies on the development of the LRFD and
534 later studies on the updated provisions for the hazard-based wind loads [3,30,57–59], while the statistics of the random
535 variables representing the uncertainties present in the geometric and material properties of a structure are based on the
536 statistics provided by Zhang et al. [9,10], which were assembled primarily from comprehensive measurement studies
537 on the variability of yield stresses, elastic moduli, cross-sectional dimensions, initial geometric imperfections, residual
538 stresses of hot-rolled sections [60–64], and are briefly described below.

539 **3.3.1 RANDOM GEOMETRIC PROPERTIES**

540 The random variable representing the initial frame out-of-plumbness imperfections ψ follows a lognormal distribution
541 with mean μ of 1/770 and standard deviation σ of 1/880 [63]. The initial member out-of-straightness imperfections
542 were modeled as a linear combination of the first 3 randomly scaled buckling modes of a single column under
543 compression $\delta(x) = \sum_{m=1}^3 a_m \sin(\pi x/L)$ where x is the coordinate along the longitudinal axis of a structural member
544 and a_m are normally distributed random scaling factors with a random sign, either positive or negative, for the m^{th}
545 buckling mode [9,10]. The statistics of the randoms scaling factors are provided in Table 1. Lastly, the variations in
546 the cross-sectional dimensions of each structural member were considered in the system reliability analyses [62]. The
547 statistics of the random variables associated with the cross-sectional dimensions of W-shaped sections are provided in
548 Table 2 with the correlation matrix provided in Table 3. The geometric uncertainties were assigned to each structural
549 member individually.

550 **3.3.2 RANDOM MATERIAL PROPERTIES**

551 In the system reliability analysis, the material assigned to the structural members was modeled using elastic-perfectly
552 plastic constitutive model with the normalized random variable associated with the elastic modulus X_E following a
553 normal distribution with a mean μ of 1.00 and a coefficient of variation V of 0.06, and the normalized random variable
554 associated with the yield stress X_{F_y} following a lognormal distribution with μ of 1.05 and V of 0.10 [60,61]. In the
555 conducted system reliability analyses, it was assumed that the material properties of all structural members were
556 perfectly correlated. However, the ECCS residual stress pattern used for each structural member was individually
557 scaled by a normally distributed random scaling factor χ with μ of 1.05 and V of 0.21 [64].

558 **3.3.3 RANDOM LOADS**

559 The normalized random variable associated with the dead load X_D follows a normal distribution with μ of 1.05 and V
560 of 0.10. The normalized random variable associated with the arbitrary point-in-time floor live load $X_{L_f}^{apt}$ follows a
561 Gamma distribution with μ of 0.22 and V of 0.54. The normalized random variable associated with the maximum
562 lifetime floor live load $X_{L_f}^{max}$ follows a Gumbel distribution with μ of 1.10 and V of 0.19. Lastly, the normalized
563 random variable associated with the maximum lifetime floor live load X_W^{max} follows a Gumbel distribution with μ of
564 0.47 and V of 0.35 [56]. It is also important to note that all system-level reliabilities reported in the subsequent sections
565 are based on the design lifetime of 50 years, corresponding to the reference period used in the ASCE 7-22 Standards,
566 consistent with the load statistics adopted from [3] and [56].

567 **3.4 IMPORTANCE SAMPLING**

568 To study the system-level reliabilities achieved by the design methods of interest for the benchmark structural steel
 569 frames, we employ *Importance Sampling* (IS), a Monte Carlo-based variance reduction technique widely adopted in
 570 structural and system reliability analysis [7,65,66], which improves the efficiency of probability of failure estimation
 571 by biasing samples towards the failure domain, thereby enabling accurate evaluation of small probabilities of failure
 572 with a significantly reduced number of samples compared to brute-force Monte Carlo simulation. In the following
 573 sections, we give a brief overview of the derivation of the numerical IS estimators for the system-level probability of
 574 failure P_f and the corresponding generalized system-level reliability index β .

575 The system-level probability of failure P_f is given by the integral of the joint probability density function (PDF) $f_{\vec{X}}(\vec{x})$
 576 of the random variables \vec{X} over the failure domain $\mathcal{F}_{\vec{X}} = \{\vec{x}: G(\vec{x}) \leq 0\}$, such that

$$P_f = \int_{\mathcal{F}_{\vec{X}}} f_{\vec{X}}(\vec{x}) d\vec{x}, \quad (28)$$

577 which is conventionally converted from the space of physical random variables \vec{X} into the space of uncorrelated
 578 standard normal random variables \vec{U} through an isoprobabilistic transformation $\vec{U} = T(\vec{X})$. The Generalized Nataf
 579 Transformation [67–69] is employed in this study, for the purpose of simplifying the development of a robust *proposal*
 580 *density function* $q(\vec{u})$, which is used to bias samples towards the failure domain. Applying this transformation, the
 581 system-level probability of failure P_f in Eq. (28) is now given by the integral of the joint PDF $\phi(\vec{u})$ of the uncorrelated
 582 standard normal random variables \vec{U} , which is known analytically, over the failure domain $\mathcal{F}_{\vec{U}} = \{\vec{u}: G(\vec{x} = T(\vec{u})) \leq$
 583 $0\}$, such that

$$P_f = \int_{\mathcal{F}_{\vec{U}}} \phi(\vec{u}) d\vec{u}. \quad (29)$$

584 Since the failure domain $\mathcal{F}_{\vec{U}}$ in the standard normal space is not known analytically, as it is a result of the nonlinear
 585 transformation $\vec{U} = T(\vec{X})$ of the failure domain $\mathcal{F}_{\vec{X}}$ in the physical space, which itself a result of the 2nd-order inelastic
 586 analysis, it is useful to introduce an indicator function $\mathbb{I}(\vec{u})$ equal to 1 if the sample \vec{u} falls within the failure domain
 587 $\mathcal{F}_{\vec{U}}$, such that $G(\vec{x} = T(\vec{u})) \leq 0$, and 0 otherwise to allow integration over the entire standard normal space.
 588 Introducing the indicator function $\mathbb{I}(\vec{u})$ and the proposal density function $q(\vec{u})$ into Eq. (29), we find that the system-
 589 level probability of failure P_f is given by the expectation of $\mathbb{I}(\vec{U})\phi(\vec{U})/q(\vec{U})$ with respect to the proposal density
 590 function $q(\vec{u})$, such that

$$P_f = \int_{\mathbb{R}^{N_{RV}}} \mathbb{I}(\vec{u})\phi(\vec{u})d\vec{u} = \int_{\mathbb{R}^{N_{RV}}} \frac{\mathbb{I}(\vec{u})\phi(\vec{u})}{q(\vec{u})}q(\vec{u})d\vec{u} = \mathbb{E}_q \left[\frac{\mathbb{I}(\vec{U})\phi(\vec{U})}{q(\vec{U})} \right]. \quad (30)$$

591 Thus, the numerical IS estimator for the system-level probability of failure P_f is given by

$$\tilde{P}_f = \frac{1}{N_S} \sum_{i=1}^{N_S} \frac{\mathbb{I}(\vec{u}_i)\phi(\vec{u}_i)}{q(\vec{u}_i)}, \quad (31)$$

592 where N_S is the number of samples \vec{u}_i generated from the proposal density function $q(\vec{u})$. The numerical IS estimator
593 for the corresponding generalized system-level reliability index β , which serves as a more familiar measure of
594 reliability, is given by

$$\tilde{\beta} = -\Phi^{-1}(\tilde{P}_f). \quad (32)$$

595 In the IS, the choice of the proposal density function $q(\vec{u})$ is crucial to ensure variance reduction of the numerical IS
596 estimators for P_f and β . As discussed by Der Kiureghian [70], a robust choice for the proposal density function $q(\vec{u})$
597 for limit state functions for series systems, such as the one given by Eq. (22), is a Gaussian mixture model with
598 multivariate standard normal components $\phi(\vec{u})$ centered at the design points $\vec{u} = \vec{u}_i^*$ of each limit state function $g_i(\vec{X})$
599 for each random load combination i , which can be obtained using the first-order reliability method (FORM), such that

$$q(\vec{u}) = \sum_{i=1}^{N_{RLC}} w_i \phi(\vec{u} - \vec{u}_i^*), \quad (33)$$

600 where w_i are the weights assigned to each component of the Gaussian mixture model satisfying the condition
601 $\sum_{i=1}^{N_{RLC}} w_i = 1$, which ensures its correct normalization. The purpose of centering the components at the design points
602 in Eq. (33) is to maximize the number of samples in the failure domain $\mathcal{F}_{\vec{y}}$. The weights w_i for the Gaussian
603 components are set to be inversely proportional to the norms of the vectors to the design points to maximize the
604 number of samples drawn in the regions of the failure domain $\mathcal{F}_{\vec{y}}$ with more probability content, such that $w_i \propto$
605 $1/|\vec{u}_i^*|$. Using these weights, we arrive at the following formulation of the proposal density function used to estimate
606 P_f in Eq. (31) and the corresponding β in Eq. (32):

$$q(\vec{u}) = \frac{\sum_{i=1}^{N_{RLC}} \phi(\vec{u} - \vec{u}_i^*)/|\vec{u}_i^*|}{\sum_{i=1}^{N_{RLC}} 1/|\vec{u}_i^*|}. \quad (34)$$

607 3.5 PROCEDURE

608 For each structural steel frame design, the system reliability analysis is conducted using the following procedure: (1)
609 FORM was performed using the improved Hasofer-Lind-Rackwitz-Fiessler method [70,71] to find the design points
610 \vec{u}_i^* of each limit state function $g_i(\vec{X})$ for each random load combination i , (2) the proposal density function $q(\vec{u})$ in
611 Eq. (34) was constructed, (3) $N_S = 10,000$ samples were generated from $q(\vec{u})$ using Latin Hypercube Sampling for
612 further variance reduction of the numerical estimators, (4) P_f was evaluated using Eq. (31) by performing N_S 2nd-order

613 inelastic analyses of the structural steel frame design, and, lastly, (5) the corresponding β was evaluated from Eq. (32).
614 Each step of the procedure was carried out using the `Fortuna.jl` package, an open-source Julia package for
615 structural and system reliability analysis [72].

616 **4 RESULTS**

617 **4.1 RESULTS OF STRUCTURAL DESIGN OPTIMIZATION**

618 The structural design optimization framework successfully identified optimal designs for all 22 benchmark structural
619 steel frames according to each design method using both proportional and nonproportional loadings, which are
620 provided in Supplementary Materials. To facilitate comparison, weight ratios relative to the designs obtained using
621 the DAM, calculated for designs obtained using either proportional or nonproportional loading, are presented in Fig.
622 3 and tabulated in Table 4. Normalizing against the DAM is appropriate, as the DAM represents the most commonly
623 used design method in U.S. practice, making these comparisons meaningful for structural engineers and highlighting
624 the potential advantages of system-based design methods. Fig. 3 demonstrates that system-based design methods –
625 AIAM, DDM90, and DDM85 – consistently produce substantially lighter structural designs compared to the
626 component-based methods – DAM and AEAM – regardless of whether proportional or nonproportional loading is
627 used during the design process with average weight reductions of 16.1(PL)/16.8(NL)% for the AIAM, 13.8/14.9% for
628 the DDM85 and 16.4/16.9% for the DDM90 when compared to the DAM. The corresponding maximum weight
629 reductions are 28.3/32.3% for the AIAM, 30.9/31.1% for the DDM85, and 32.1%/31.5% for the DDM90. In general,
630 the DAM and AEAM design methods result in nearly identical weights for all frames, while the AIAM and DDM90
631 result in the lightest designs, closely followed by DDM85, which is only slightly heavier. These trends remain
632 consistent across all structural steel frames, indicating that the weight reduction benefits of system-based design
633 methods are robust to variations in structural configurations and loading conditions.

634 The comparison of the weights of the optimal designs obtained using proportional and nonproportional loadings,
635 presented in Fig. 4, demonstrates that, for the component-based design methods, there is minimal difference in the
636 resulting weights between the two types of loadings, indicating that these design methods are relatively insensitive to
637 how the loads are applied during the design process. In contrast, for the system-based design methods, using
638 nonproportional loading can lead to modestly lighter designs compared to proportional loading in some cases, though,
639 on average, the difference remains relatively small across all the analyzed structural steel frames: 1.3% for the AIAM,
640 1.7% for the DDM85, and 0.9% for the DDM90.

4.2 RESULTS OF SYSTEM RELIABILITY ANALYSIS

Performing the system reliability analyses that included uncertainties in geometric properties, material properties, and applied loads using the Importance Sampling technique for each optimal structural steel frame design, the system-level reliability indices β presented in Table 5 were obtained. These values of β provide a robust quantitative basis for comparing the system-level reliabilities achieved by the design methods of interest relative to each other and the target levels of reliability specified in design codes. For example, a target reliability index β_t of 3.0 is recommended in the ASCE 7-22 Standard for Risk Category II buildings utilizing performance-based design procedures (Table 1.3-1). The structural member strength provisions of the AISC 360-22 Specification generally targeted β_t of 3.0, but allowed values as low as 2.6, while the provisions of the AISI S100-24 Specification [73] were calibrated to β_t of 2.5 for members and 3.5 for connections. For comparison purposes, system-level target reliabilities β_t of 2.5 and 3.0 are highlighted herein. Final selection of target levels of system reliability requires input from design code committees and professionals.

To facilitate comparison, β values of the optimal designs obtained according to the requirements of each design method of interest are presented in Fig. 5. The component-based design methods – DAM and AEAM – result in β values that exceed β_t of 3.0 for 20 out of 22 frames for the DAM and 18 out of 22 frames for the AEAM, with mean β values ranging between 3.65 and 3.75, reflecting a conservative margin in reliability as they ensure reliability on the level of individual structural components without consideration of the potential for significant force redistribution as a system or its significant portion reaches a strength limit state. In contrast, the system-based design methods – AIAM and DDM – overall result in β values that fall closer to β_t of 3.0. This trend is evident from the mean β values reported in Table 5, which range from 2.8 to 3.1, as well as from the substantially reduced variability, with V decreasing from 18.7-20.6% for the component-based design methods to 6.1-9.9% for the system-based design methods. This highlights the efficiency of system-based design methods in material utilization while also emphasizing the need for careful calibration to ensure that target levels of reliability are consistently met.

The comparison between β values of the optimal designs obtained using proportional and nonproportional loadings, is presented in Fig. 6, demonstrates that the designs obtained using proportional loading are more reliable than the designs obtained using nonproportional loading, especially for the system-based design methods, which is consistent with the fact that system-based design methods result in lighter designs as observed in Fig. 4.

5 SENSITIVITY OF ADVANCED INELASTIC ANALYSIS METHOD

As observed in Fig. 5, the AIAM with the reduction factor of 0.90 for E and F_y as currently specified in Appendix 1 of the AISC 360-22 Specification, referred to as the AIAM90, consistently resulted in β values around 2.85. To understand the sensitivity of the design method to the selected reductions we considered a modest recalibration of the reduction factor, through an additional set of optimal designs obtained according to the AIAM, but with a more conservative reduction factor on E and F_y of 0.85, referred to as AIAM85. The resulting weights and system-level reliability indices of the optimal designs are presented in Table 6.

Comparing β values between the AIAM85 and AIAM90, shown in Fig. 7, we can observe that using the reduction factor of 0.85 leads to an increase in β values, as reflected by an increase in the mean β values from 2.85 (Table 5) to 3.15 (Table 6) – this represents a roughly threefold reduction in the mean P_f values from 2.2×10^{-3} to 8.2×10^{-4} . This change is achieved at the cost of slightly heavier designs, with an average weight increase of 3.4%, as shown in Fig. 8, when compared to the AIAM90. When compared to the DAM, AIAM90 provides weight savings of 16.1/16.8% and AIAM85 provides weight savings of 13.3/14.0%. Overall, this sensitivity exercise demonstrates that modest changes in the reduction factor can have positive influence on the system-level reliability while still maintaining material efficiency.

6 DISCUSSION

This study examines system-level reliabilities achieved by two component-based design methods and two system-based design methods for a series of benchmark structural steel frames using a combined framework of structural design optimization and system reliability analysis. The results demonstrate clear and systematic differences between the two categories of design methods in terms of achieved reliability, variability, and material efficiency.

The component-based design methods – DAM and AEAM – consistently produced designs with β values exceeding β_t of 3.0, with mean β values ranging between 3.65 and 3.75, and high variability as reflected by V values ranging from 18.7 to 20.6%. This trend reflects the inherently conservative nature of component-based design, in which reliability is enforced at the level of first individual structural members, and the potential for inelastic force redistribution is not accounted for. In contrast, the system-based design methods – AIAM and DDM – produced significantly lighter designs, highlighting their material and economic efficiency, with β values that were generally closer to β_t of 3.0 and exhibited substantially lower variability; for these design methods, mean β values ranged between 2.8 and 3.1, with V values ranging from 6.1 to 9.9%. The low variability reflects more consistent system-

696 level reliability outcomes enabled by explicit consideration of beneficial inelastic load redistribution effects. These
697 improvements in system-level reliabilities are accompanied by significant reductions in structural weight. Relative to
698 the DAM, the average weight reduction of 16.1/16.8% was achieved for the AIAM, 13.8/14.9% for the DDM85 and
699 16.4/16.9% for the DDM90. These results demonstrate that system-based design methods achieve lower structural
700 weights not by sacrificing safety, but by allocating material more efficiently at the system level, thereby reducing
701 excess conservatism inherent in component-based design methods.

702 The results also indicate that, similar to DDM90, the system-level reliabilities of AIAM designs, when implemented
703 using the reduction factor of 0.90 specified in Appendix 1 of the AISC 360-22 Specification (AIAM90), frequently
704 fall below β_t of 3.0. This observation motivated a modest sensitivity study of the AIAM's reduction factor. Using a
705 reduction factor of 0.85 (AIAM85) resulted in an increase in the mean β values from approximately 2.85 to 3.15. This
706 improvement was achieved with a modest average weight increase of only 3.4% relative to AIAM90. Despite this
707 increase, AIAM85 designs remain substantially more materially efficient than component-based designs, retaining
708 weight reductions of 13.3/14.0% relative to DAM, compared to 16.1/16.7% for AIAM90. These results demonstrate
709 that a modest changes in the reduction factor can have robust changes on the system-level reliability while largely
710 preserving significant weight reduction benefits.

711 The findings of this study demonstrate a clear trade-off between the weight of a structure and its system-level
712 reliability. System-based design methods offer a path towards more materially efficient designs of structural steel
713 buildings by capturing, although complex, beneficial inelastic load redistribution effects omitted in component-based
714 methods. However, this advantage comes with the caveat that these design methods require careful calibration of the
715 embedded reduction factors to achieve adequate levels of safety.

716 **7 CONCLUSION**

717 In this study, a general framework for evaluating the system-level reliability of arbitrary steel structures designed using
718 any arbitrary design method was developed. The framework is based on the use of a structural design optimization
719 framework employing the Genetic Algorithm to identify optimal designs with least possible weights, combined with
720 a robust system reliability analysis employing the Importance Sampling technique to account for uncertainties in
721 geometric properties, material properties, and applied loads to accurately evaluate the system-level reliabilities.
722 Applying this framework to 22 benchmark structural steel frames, the study yields the following major findings:

- 723 - Component-based design methods –Direct Analysis Method and Advanced Elastic Analysis Method –
724 consistently produce designs with high mean system-level reliability index values between 3.65 and 3.75,
725 and high variability (coefficient of variation of 18.7-20.6%). This conservatism reflects the fact that these
726 design methods ensure reliability at the level of individual components without explicit consideration of
727 beneficial inelastic load redistribution.
- 728 - System-based design methods – Advanced Inelastic Analysis Method and Direct Design Method – produce
729 significantly lighter designs, with average weight reductions of 13-17% relative to the Direct Analysis
730 Method, and more consistent mean system-level reliability index values between 2.8 and 3.1, and
731 substantially lower variability (coefficient of variation of 6.1-9.9%), reflecting much more efficient use of
732 material without compromising safety.
- 733 - The Advanced Inelastic Analysis Method, as currently specified in Appendix 1 of the AISC 360-22
734 Specification with a material reduction factor of 0.90, yields structural steel frame designs with the mean
735 system reliability index value of 2.85. It was shown that a modest change in the reduction factor to 0.85 raises
736 the mean system reliability index to approximately 3.15 at the cost of an average weight increase of only
737 3.4%, demonstrating that a modest recalibrations can meaningfully improve safety while preserving material
738 efficiency.

739 *Limitations and Future Work.* The findings of this study are subject to the following limitations, which should be
740 considered when interpreting the results and extending them to practice: (1) the study is restricted to planar structural
741 steel frames with compact and non-slender W-shaped sections, and results may not generalize directly to spatial
742 structures, non-compact sections, or other cross-sectional types, (2) only strength-based limit states are considered –
743 serviceability limit states, including interstory drift, peak roof displacement, and member rotation capacity, are not
744 included, and since serviceability requirements frequently govern the design of low- to mid-rise frames, the system-
745 level reliabilities reported here represent lower bounds on those achievable in designs by serviceability-based limit
746 states, (3) more broadly, the system-level reliability indices reported here are lower bounds that correspond to strength-
747 governed designs, and any source of overstrength, whether arising from serviceability-governed design, practical
748 constraints on section availability, or engineering conservatism, will result in higher system-level reliabilities than
749 those reported, (4) roof live loads and floor live loads are treated as statistically identical, an assumption adopted for
750 consistency with prior calibration studies but one that recent work suggests may be overly conservative [42,43], (5)

751 connections are idealized as either perfectly rigid or perfectly pinned, and the effects of partial restraint are not
752 considered, and (6) the load statistics and load combinations are based on ASCE 7-22 Standard, and the findings may
753 differ when AS/NZS or Eurocode load models are used. Each of these limitations represents a natural direction for
754 future research and addressing them would broaden the applicability of the proposed framework and strengthen the
755 basis for the adoption of system-based design methods in future design codes.

756 *Recommendations for Implementation in Design Codes.* For system-based design methods to be broadly adopted in
757 future design codes, three steps are recommended. First, the calibration of system-level resistance factors must be
758 extended beyond the planar frame configurations studied here to encompass a wider range of structural archetypes,
759 including spatial frames, braced frames, and frames with non-compact sections. Second, design code committees
760 should reach explicit agreement on an appropriate target system-level target reliability index – a value in the range of
761 2.5 to 3.0 appears consistent with the results of this and prior studies, but the final selection must account for system
762 type, degree of redundancy, and the definition of system failure adopted. Third, practical guidance must be developed
763 for practitioners on the modeling of stress-strength curves and geometric and material imperfections, the selection of
764 material reduction factors, and the interpretation of system-level strength checks in the context of everyday design
765 workflows.

766 *Path to Broader Adoption.* The structural design optimization and system reliability analysis frameworks developed
767 in this study provide reproducible and generalizable tools for future calibration studies targeting these goals. The use
768 of open-source software (OpenSeesPy for finite element analysis, `Metaheuristics.jl` for structural design
769 optimization, and `Fortuna.jl` for system reliability analysis) enables independent verification and extension by
770 other researchers and design code developers, and supports the continued advancement of system-based design
771 methods in future design codes for structural steel buildings.

772 **DATA AVAILABILITY STATEMENT**

773 Some or all data, models, or code that support the findings of this study are available from the corresponding author
774 upon reasonable request.

775 **ACKNOWLEDGEMENTS**

776 The authors would like to thank the American Institute of Steel Construction for the financial support of the “*System*
777 *Reliability of Steel Structures*” project. The authors would also like to thank Dr. Jesús-Adolfo Mejía-de-Dios and Dr.
778 Efrén Mezura-Montes from the University of Veracruz for developing the `Metaheuristics.jl` package and

779 providing invaluable support in its application. The first author would also like to personally thank fellow graduate
780 students Saroj Khanal and Tomás Tapia from the Johns Hopkins University for insightful discussions on the discrete
781 optimization problems with nonlinear constraints. Lastly, the first author would also like to thank Kyurae Kim, a
782 graduate student from the University of Pennsylvania, who provided valuable tips on generating samples from
783 Gaussian mixture models using the Latin Hypercube Sampling technique and improving the stability of the
784 implementation of the Generalized Nataf Transformation in the `Fortuna.jl` package.

785 SUPPLEMENTARY MATERIALS

786 The supplementary materials are available at the following URL:

787 <https://archive.data.jhu.edu/previewurl.xhtml?token=ad5901e7-15c0-40f2-8844-f835f40b54f3>.

788 REFERENCES

- 789 [1] AISC, ANSI/AISC 360-22: Specification for Structural Steel Buildings, (2022).
790 [2] AISC, AISC: Standard Specification, (1923).
791 [3] B.R. Ellingwood, T.V. Galambos, J.G. MacGregor, C.A. Cornell, Development of a Probability Based Load Criterion for
792 American National Standard A58, National Bureau of Standards, Washington, DC, 1980.
793 [4] T.V. Galambos, Load and Resistance Factor Design, Engineering Journal (1981).
794 [5] R.D. Ziemian, W. McGuire, G.G. Deierlein, Inelastic Limit States Design. Part I: Planar Frame Studies, J. Struct. Eng. 118
795 (1992) 2532–2549. [https://doi.org/10.1061/\(ASCE\)0733-9445\(1992\)118:9\(2532\)](https://doi.org/10.1061/(ASCE)0733-9445(1992)118:9(2532)).
796 [6] R.D. Ziemian, W. McGuire, G.G. Dierlein, Inelastic Limit States Design Part II: Three-Dimensional Frame Study, J.
797 Struct. Eng. 118 (1992) 2550–2568. [https://doi.org/10.1061/\(ASCE\)0733-9445\(1992\)118:9\(2550\)](https://doi.org/10.1061/(ASCE)0733-9445(1992)118:9(2550)).
798 [7] S.G. Buonopane, B.W. Schafer, Reliability of Steel Frames Designed with Advanced Analysis, J. Struct. Eng. 132 (2006)
799 267–276. [https://doi.org/10.1061/\(ASCE\)0733-9445\(2006\)132:2\(267\)](https://doi.org/10.1061/(ASCE)0733-9445(2006)132:2(267)).
800 [8] S. Shayan, System Reliability-Based Design of 2D Steel Frames by Advanced Analysis, University of Sydney, 2013.
801 [9] H. Zhang, S. Shayan, K.J.R. Rasmussen, B.R. Ellingwood, System-Based Design of Planar Steel Frames, I: Reliability
802 Framework, Journal of Constructional Steel Research 123 (2016) 135–143. <https://doi.org/10.1016/j.jcsr.2016.05.004>.
803 [10] H. Zhang, S. Shayan, K.J.R. Rasmussen, B.R. Ellingwood, System-Based Design of Planar Steel Frames, II: Reliability
804 Results and Design Recommendations, Journal of Constructional Steel Research 123 (2016) 154–161.
805 <https://doi.org/10.1016/j.jcsr.2016.05.005>.
806 [11] I. Arrayago, K.J.R. Rasmussen, H. Zhang, System-Based Reliability Analysis of Stainless Steel Frames Subjected to
807 Gravity and Wind Loads, Structural Safety 97 (2022) 102211. <https://doi.org/10.1016/j.strusafe.2022.102211>.
808 [12] I. Arrayago, K.J.R. Rasmussen, Reliability of Stainless Steel Frames Designed Using the Direct Design Method in
809 Serviceability Limit States, Journal of Constructional Steel Research 196 (2022) 107425.
810 <https://doi.org/10.1016/j.jcsr.2022.107425>.
811 [13] AISC, AISC: Manual of Steel Construction, (1967).
812 [14] AISC, AISC: Load and Resistance Factor Design Specification for Structural Steel Buildings, (1986).
813 [15] A.E. Maleck, Second-Order Inelastic and Modified Elastic Analysis and Design Evaluation of Planar Steel Frames,
814 Georgia Institute of Technology, 2001.
815 [16] G.G. Deierlein, J.F. Hajjar, J.A. Yura, D.W. White, W.F. Baker, Proposed New Provisions for Frame Stability Using
816 Second-Order Analysis, in: Proceedings of the Annual Stability Conference, Structural Stability Research Council, Seattle,
817 WA, 2002.
818 [17] J.M. Martinez-Garcia, Benchmark Studies to Evaluate New Provisions for Frame Stability Using Second-Order Analysis,
819 Bucknell University, 2002.
820 [18] A.E. Maleck, D.W. White, Direct Analysis Approach for the Assessment of Frame Stability: Verification Studies, in:
821 Proceedings of the Annual Stability Conference, Structural Stability Research Council, Baltimore, MD, 2003.
822 [19] A.E. Surovek-Maleck, D.W. White, Alternative Approaches for Elastic Analysis and Design of Steel Frames. I: Overview,
823 J. Struct. Eng. 130 (2004) 1186–1196. [https://doi.org/10.1061/\(ASCE\)0733-9445\(2004\)130:8\(1186\)](https://doi.org/10.1061/(ASCE)0733-9445(2004)130:8(1186)).
824 [20] A.E. Surovek-Maleck, D.W. White, Alternative Approaches for Elastic Analysis and Design of Steel Frames. II:
825 Verification Studies, J. Struct. Eng. 130 (2004) 1197–1205. [https://doi.org/10.1061/\(ASCE\)0733-9445\(2004\)130:8\(1197\)](https://doi.org/10.1061/(ASCE)0733-9445(2004)130:8(1197)).
826 [21] J.M. Martinez-Garcia, R.D. Ziemian, Benchmark Studies to Compare Frame Stability Provisions, in: Proceedings of the
827 Annual Stability Conference, Structural Stability Research Council, San Antonio, TX, 2006.
828 [22] AISC, ANSI/AISC 360-05: Specification for Structural Steel Buildings, (2005).

829 [23] Y. Wang, R.D. Ziemian, Design by Advanced Elastic Analysis: An Investigation of Beam-Columns Resisting Minor-Axis
830 Bending, in: Proceedings of the Annual Stability Conference, Structural Stability Research Council, St. Louis, MO, 2019.

831 [24] Y. Wang, R.D. Ziemian, Design by Advanced Elastic Analysis: An Investigation of Beam-Columns, Eng J 58 (2021) 123–
832 137. <https://doi.org/10.62913/engj.v58i2.1174>.

833 [25] M.T. Nwe Nwe, The Modified Direct Analysis Method: An Extension of the Direct Analysis Method, Bucknell University,
834 2014.

835 [26] E.J. Giensen Loo, Design of Steel Structures by Advanced Second-Order Elastic Analysis: Background Studies, Bucknell
836 University, 2016.

837 [27] AISC, ANSI/AISC 360-16: Specification for Structural Steel Buildings, (2016).

838 [28] AISC, ANSI/AISC 360-10: Specification for Structural Steel Buildings, (2010).

839 [29] L.S. Beedle, Plastic Design of Steel Frames, Wiley, New York, 1970.

840 [30] ASCE, ASCE 7-22: Minimum Design Loads and Associated Criteria for Buildings and Other Structures, (2021).

841 [31] Standards Australia, AS/NZS 1170.0 - Structural Design Actions, Part 0: General Principles, (2002).

842 [32] Standards Australia, AS/NZS 1170.1 - Structural Design Actions, Part 1: Permanent, Imposed and Other Actions, (2002).

843 [33] Standards Australia, DR AS 4100 - Steel Structures (Draft), (2026).

844 [34] Standards Australia, AS/NZS 4600 - Cold-Formed Steel Structures, (2018).

845 [35] Standards Australia, AS 4084.1 - Steel Storage Racking, Part 1: Design, (2023).

846 [36] Standards Australia, AS 3610.2 - Formwork for Concrete, Part 2: Design and Construction, (2023).

847 [37] C.W. Ziemian, R.D. Ziemian, Efficient Geometric Nonlinear Elastic Analysis for Design of Steel Structures: Benchmark
848 Studies, Journal of Constructional Steel Research 186 (2021) 106870. <https://doi.org/10.1016/j.jcsr.2021.106870>.

849 [38] W. Liu, System Reliability-Based Design of Three-Dimensional Steel Structures by Advanced Analysis, University of
850 Sydney, 2016.

851 [39] W. Liu, H. Zhang, K.J.R. Rasmussen, S. Yan, System-Based Limit State Design Criterion for 3D Steel Frames Under
852 Wind Loads, Journal of Constructional Steel Research 157 (2019) 440–449. <https://doi.org/10.1016/j.jcsr.2019.02.015>.

853 [40] H. Zhang, H. Liu, B.R. Ellingwood, K.J.R. Rasmussen, System Reliabilities of Planar Gravity Steel Frames Designed by
854 the Inelastic Method in AISC 360-10, J. Struct. Eng. 144 (2018) 04018011. [https://doi.org/10.1061/\(ASCE\)ST.1943-541X.0001991](https://doi.org/10.1061/(ASCE)ST.1943-541X.0001991).

855 [41] D. Akchurin, S. Ádány, R.D. Ziemian, K.J.R. Rasmussen, B.W. Schafer, System-Based Design Methods: Stability and
856 Reliability of Benchmark Structural Steel Frames, in: Proceedings of the Annual Stability Conference, Structural Stability
857 Research Council, Louisville, KY, 2025.

858 [42] A. Karasu, K.D. Peterman, S.R. Arwade, Analysis of Roof Live Loads in Industrial Buildings, in: Proceedings of the Cold-
859 Formed Steel Research Consortium Colloquium, 2022.

860 [43] A. Karasu, K.D. Peterman, S.R. Arwade, Roof Live Loads for Low-Slope Roofs, J. Struct. Eng. 151 (2025) 04025064.
861 <https://doi.org/10.1061/JSENDH.STENG-14363>.

862 [44] AISC, AISC: Steel Construction Manual, (2023).

863 [45] H. Liu, System Reliability Calibrations for the Direct Design Method of Planar Steel Frames with Partially Restrained
864 Connections, University of Sydney, 2019.

865 [46] C. Zhu, K.J.R. Rasmussen, S. Yan, Generalised Component Model for Structural Steel Joints, Journal of Constructional
866 Steel Research 153 (2019) 330–342. <https://doi.org/10.1016/j.jcsr.2018.10.026>.

867 [47] S. Yan, K.J.R. Rasmussen, Generalised Component Method-Based Finite Element Analysis of Steel Frames, Journal of
868 Constructional Steel Research 187 (2021) 106949. <https://doi.org/10.1016/j.jcsr.2021.106949>.

869 [48] D.E. Goldberg, Genetic Algorithms in Search, Optimization, and Machine Learning, 30. print, Addison-Wesley, Boston,
870 2012.

871 [49] J.-A. Mejía-de-Dios, E. Mezura-Montes, Metaheuristics.jl: A Julia Package for Single- and Multi-Objective Optimization,
872 JOSS 7 (2022) 4723. <https://doi.org/10.21105/joss.04723>.

873 [50] K. Deb, An Efficient Constraint Handling Method for Genetic Algorithms, Computer Methods in Applied Mechanics and
874 Engineering 186 (2000) 311–338. [https://doi.org/10.1016/S0045-7825\(99\)00389-8](https://doi.org/10.1016/S0045-7825(99)00389-8).

875 [51] K. Deb, R.B. Agrawal, Simulated Binary Crossover for Continuous Search Space, Complex Systems 9 (1995) 115–148.

876 [52] K. Deb, A. Deb, Analysing Mutation Schemes for Real-Parameter Genetic Algorithms, IJAISC 4 (2014) 1.
877 <https://doi.org/10.1504/IJAISC.2014.059280>.

878 [53] F. McKenna, M.H. Scott, G.L. Fenves, Nonlinear Finite-Element Analysis Software Architecture Using Object
879 Composition, J. Comput. Civ. Eng. 24 (2010) 95–107. [https://doi.org/10.1061/\(ASCE\)CP.1943-5487.0000002](https://doi.org/10.1061/(ASCE)CP.1943-5487.0000002).

880 [54] C.J. Turkstra, H.O. Madsen, Load Combinations in Codified Structural Design, J. Struct. Div. 106 (1980) 2527–2543.
881 <https://doi.org/10.1061/JSDEAG.0005599>.

882 [55] T. McAllister, R. Zheng Guo, J.Y. Lee, eds., Structural Reliability Guidance in ASCE 7-22: Principles and Methods,
883 American Society of Civil Engineers, Reston, VA, 2025.

884 [56] D. Akchurin, R. Sabelli, R.D. Ziemian, B.W. Schafer, ASD and LRFD: Reliability Comparison for Designs Subjected to
885 Wind Loads, Journal of Constructional Steel Research 213 (2024) 108327. <https://doi.org/10.1016/j.jcsr.2023.108327>.

886 [57] B. Ellingwood, J.G. MacGregor, T.V. Galambos, C.A. Cornell, Probability Based Load Criteria: Load Factors and Load
887 Combinations, J. Struct. Div. 108 (1982) 978–997. <https://doi.org/10.1061/JSDEAG.0005959>.

888 [58] T.V. Galambos, B. Ellingwood, J.G. MacGregor, C.A. Cornell, Probability Based Load Criteria: Assessment of Current
889 Design Practice, J. Struct. Div. 108 (1982) 959–977. <https://doi.org/10.1061/JSDEAG.0005958>.

891 [59] T.P. McAllister, N. Wang, B.R. Ellingwood, Risk-Informed Mean Recurrence Intervals for Updated Wind Maps in ASCE
892 7-16, J. Struct. Eng. 144 (2018) 06018001. [https://doi.org/10.1061/\(ASCE\)ST.1943-541X.0002011](https://doi.org/10.1061/(ASCE)ST.1943-541X.0002011).

893 [60] T.V. Galambos, M.K. Ravindra, Properties of Steel for Use in LRFD, J. Struct. Div. 104 (1978) 1459–1468.
894 <https://doi.org/10.1061/JSDEAG.0004988>.

895 [61] F.M. Bartlett, R.J. Dexter, M.D. Graeser, J.J. Jelinek, B.J. Schmidt, T.V. Galambos, Updating Standard Shape Material
896 Properties Database for Design and Reliability, Eng J 40 (2003) 2–14. <https://doi.org/10.62913/engi.v40i1.800>.

897 [62] J. Melcher, Z. Kala, M. Holický, M. Fajkus, L. Rozlívka, Design Characteristics of Structural Steels Based on Statistical
898 Analysis of Metallurgical Products, Journal of Constructional Steel Research 60 (2004) 795–808.
899 [https://doi.org/10.1016/S0143-974X\(03\)00144-5](https://doi.org/10.1016/S0143-974X(03)00144-5).

900 [63] S. Shayan, K.J.R. Rasmussen, H. Zhang, On the Modelling of Initial Geometric Imperfections of Steel Frames in
901 Advanced Analysis, Journal of Constructional Steel Research 98 (2014) 167–177.
902 <https://doi.org/10.1016/j.jcsr.2014.02.016>.

903 [64] S. Shayan, K.J.R. Rasmussen, H. Zhang, Probabilistic Modelling of Residual Stress in Advanced Analysis of Steel
904 Structures, Journal of Constructional Steel Research 101 (2014) 407–414. <https://doi.org/10.1016/j.jcsr.2014.05.028>.

905 [65] R.E. Melchers, Importance Sampling in Structural Systems, Structural Safety 6 (1989) 3–10. [https://doi.org/10.1016/0167-4730\(89\)90003-9](https://doi.org/10.1016/0167-4730(89)90003-9).

906 [66] Y. Ibrahim, Observations on Applications of Importance Sampling in Structural Reliability Analysis, Structural Safety 9
907 (1991) 269–281. [https://doi.org/10.1016/0167-4730\(91\)90049-F](https://doi.org/10.1016/0167-4730(91)90049-F).

908 [67] A. Nataf, Étude Graphique De Détermination De Distributions De Probabilités Planes Dont Les Marges Sont Données,
909 Comptes Rendus de l'Académie des Sciences 225 (1962) 42–43.

910 [68] R. Lebrun, A. Dutfoy, A Generalization of the Nataf Transformation to Distributions with Elliptical Copula, Probabilistic
911 Engineering Mechanics 24 (2009) 172–178. <https://doi.org/10.1016/j.probengmech.2008.05.001>.

912 [69] R. Lebrun, A. Dutfoy, An Innovating Analysis of the Nataf Transformation from the Copula Viewpoint, Probabilistic
913 Engineering Mechanics 24 (2009) 312–320. <https://doi.org/10.1016/j.probengmech.2008.08.001>.

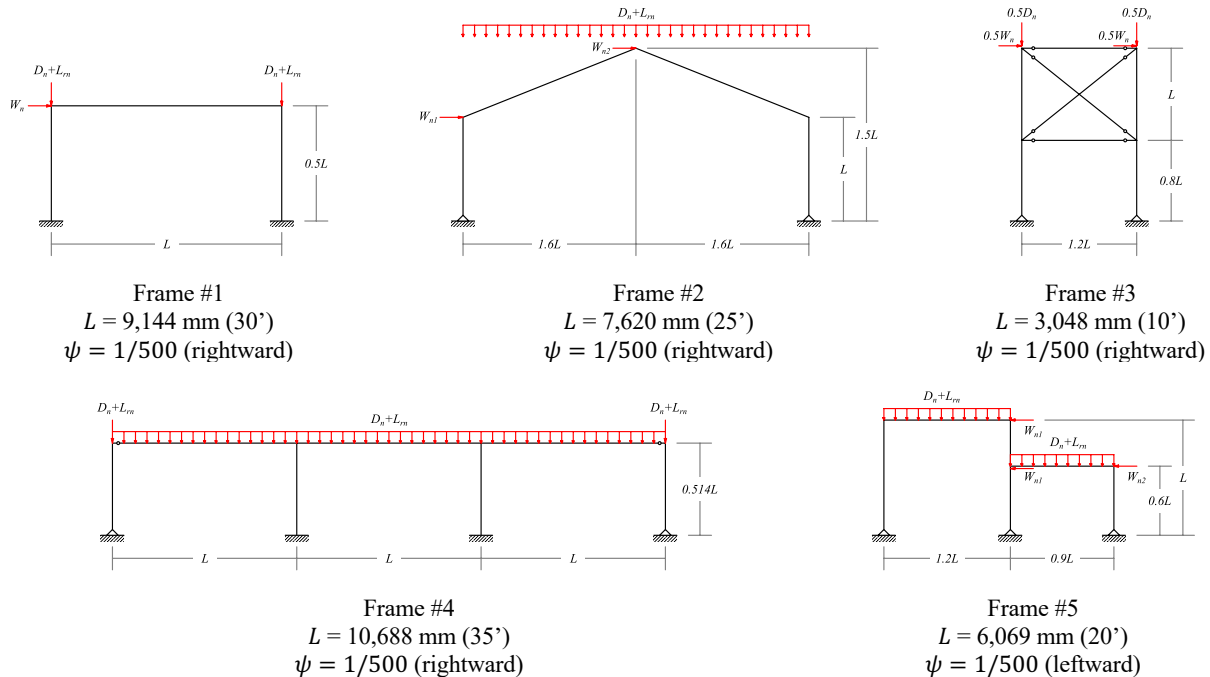
914 [70] A. Der Kiureghian, Structural and System Reliability, Cambridge University Press, Cambridge, 2022.
915 <https://doi.org/10.1017/9781108991889>.

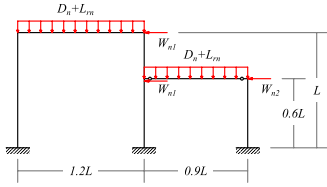
916 [71] P.-L. Liu, A. Der Kiureghian, Optimization Algorithms for Structural Reliability Analysis, University of California
917 Berkley, Berkley, CA, 1986. <https://escholarship.org/uc/item/1kg0q03z>.

918 [72] D. Akchurin, Fortuna.jl: Structural and System Reliability Analysis in Julia, JOSS 9 (2024) 6967.
919 <https://doi.org/10.21105/joss.06967>.

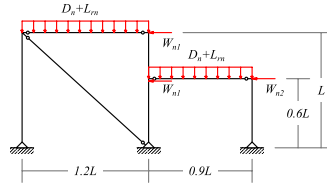
920 [73] ANSI/SDI, ANSI/SDI AISI S100-2024: North American Specification for the Design of Cold-Formed Steel Structural
921 Members, (2024).
922

923 FIGURES

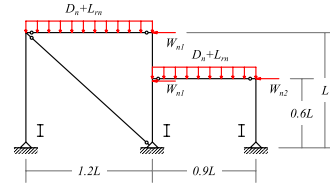




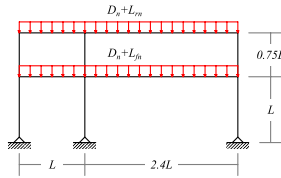
Frame #6
 $L = 6,069 \text{ mm (20')}$
 $\psi = 1/500 \text{ (leftward)}$



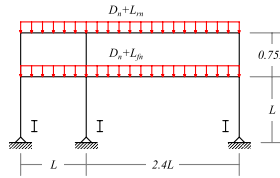
Frame #7
 $L = 6,069 \text{ mm (20')}$
 $\psi = 1/500 \text{ (leftward)}$



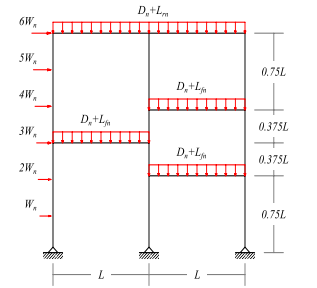
Frame #8
 $L = 6,069 \text{ mm (20')}$
 $\psi = 1/500 \text{ (leftward)}$



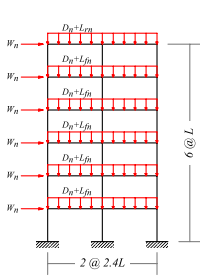
Frame #9
 $L = 6,069 \text{ mm (20')}$
 $\psi = 1/500 \text{ (leftward)}$



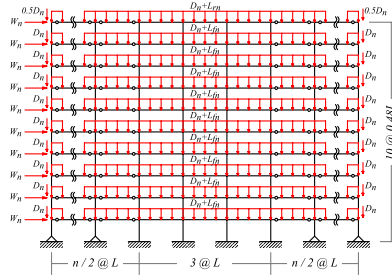
Frame #10
 $L = 6,069 \text{ mm (20')}$
 $\psi = 1/500 \text{ (leftward)}$



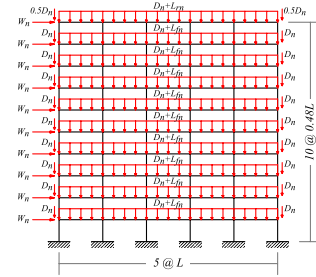
Frame #11
 $L = 6,069 \text{ mm (20')}$
 $\psi = 1/500 \text{ (rightward)}$



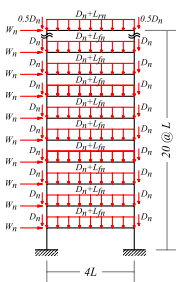
Frame #12
 $L = 3,750 \text{ mm (12.3')}$
 $\psi = 1/500 \text{ (rightward)}$



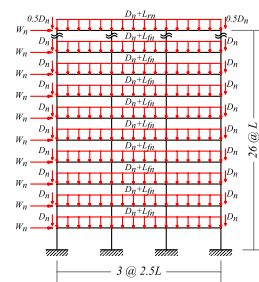
Frames #13 to #16
 $L = 6,069 \text{ mm (20')}$
 $\psi = 1/500 \text{ (rightward)}$
 $n = \{0, 4, 8, 12\} \text{ lean-on columns}$



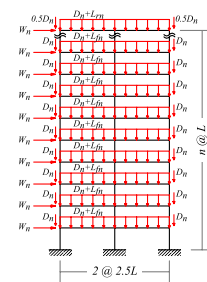
Frame #17
 $L = 6,069 \text{ mm (20')}$
 $\psi = 1/500 \text{ (rightward)}$



Frame #18
 $L = 4,267 \text{ mm (14')}$
 $\psi = 1/500 \text{ (rightward)}$

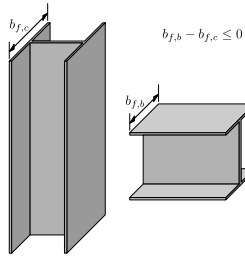


Frame #19
 $L = 3,658 \text{ mm (12')}$
 $\psi = 1/500 \text{ (rightward)}$

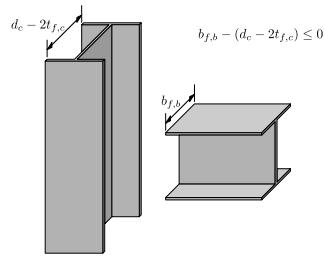


Frames #20 to #22
 $L = 3,658 \text{ mm (12')}$
 $\psi = 1/500 \text{ (rightward)}$
 $n = \{30, 30, 40\} \text{ stories}$

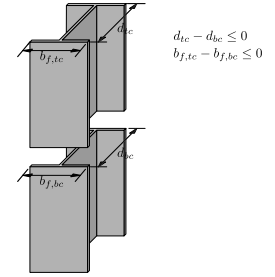
Fig. 1: Benchmark structural steel frames.



(a) Beam-to-column connections:
Column bending about major axis

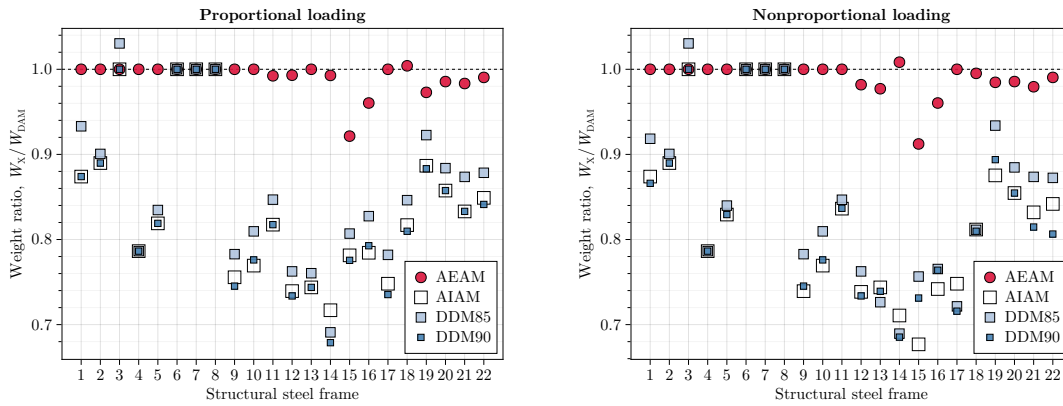


(b) Beam-to-column connections:
Column bending about minor axis
Fig. 2: Constructability constraints.



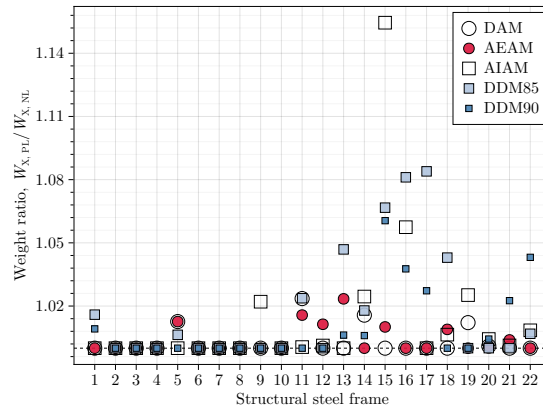
(c) Column-to-column connections

925



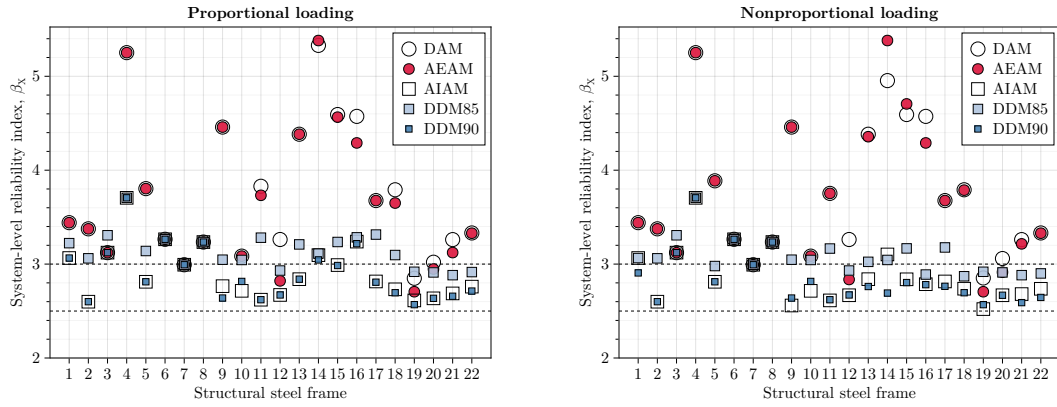
926

927 Fig. 3: Weights ratios between the optimal designs obtained using the design methods of interest
928 using the DAM.



929

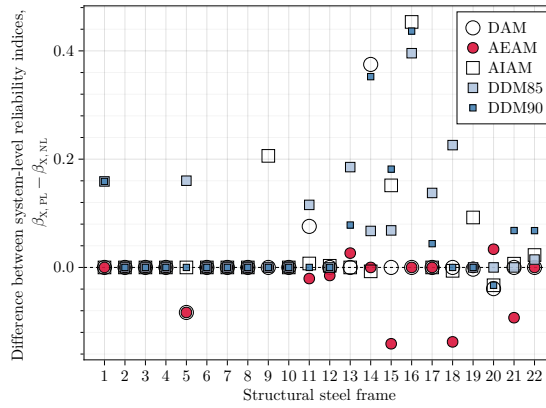
930 Fig. 4: Weights ratios between the optimal designs obtained using proportional and nonproportional loadings.



931

932

Fig. 5: System-level reliability indices of the optimal designs obtained using the design methods of interest.

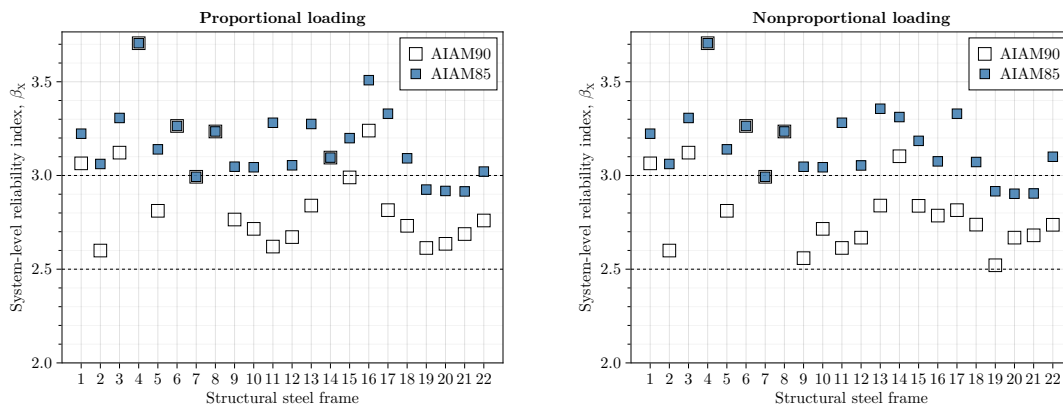


933

934

935

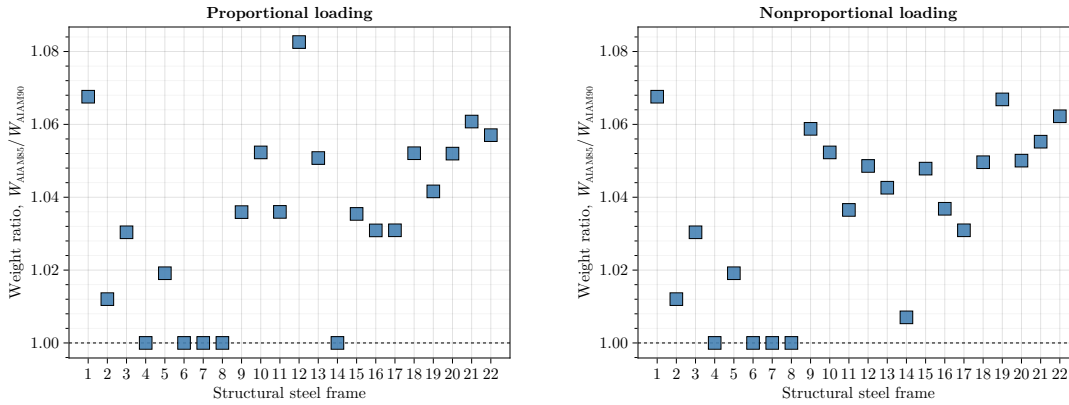
Fig. 6: Difference between the system-level reliability indices of the optimal designs obtained using the proportional and nonproportional loading.



936

937

Fig. 7: System reliability indices of the optimal designs obtained using the AIAM with the reduction factors of 0.85 and 0.90.



938

939 Fig. 8: Weights ratios between the optimal designs obtained using the AIAM with the reduction factors of 0.85 and 0.90.

940 **TABLES**

941

Table 1. Statistics of the random scaling factors.

Random scaling factor	Distribution	Mean, μ	Standard deviation, σ
a_1/L	Normal	0.000556	0.000427
a_2/L	Normal	0.000139	0.000071
a_3/L	Normal	0.000073	0.000078

942

Table 2. Statistics of the random variables associated the cross-sectional dimensions of W-shaped sections.

Dimension	Distribution	Mean, μ	Coefficient of variation, V
Depth, d/d_n	Normal	1.001	0.0044
Flange width, $b_{f1}/b_{f1,n}$	Normal	1.012	0.0100
Flange width, $b_{f2}/b_{f2,n}$	Normal	1.015	0.0095
Web thickness, $t_w/t_{w,n}$	Normal	1.055	0.0400
Flange thickness, $t_{f1}/t_{f1,n}$	Normal	0.988	0.0440
Flange thickness, $t_{f2}/t_{f2,n}$	Normal	0.988	0.0490

943

Table 3. Correlation matrix of the random variables associated the cross-sectional dimensions of W-shaped sections.

Dimension	d/d_n	$b_{f1}/b_{f1,n}$	$b_{f2}/b_{f2,n}$	$t_w/t_{w,n}$	$t_{f1}/t_{f1,n}$	$t_{f2}/t_{f2,n}$
d/d_n	1	-0.0068	+0.0534	+0.0399	-0.0686	-0.0989
$b_{f1}/b_{f1,n}$		1	+0.6227	-0.2142	-0.2681	-0.1456
$b_{f2}/b_{f2,n}$			1	-0.2132	-0.1596	-0.0423
$t_w/t_{w,n}$				1	+0.2368	+0.2451
$t_{f1}/t_{f1,n}$					1	+0.7634
$t_{f2}/t_{f2,n}$						1

Note that the original study by Melcher et al. (2004) as well as the study by Zhang et al. (2016a) erroneously report this correlation matrix with non-symmetric upper and lower triangular parts. In this study, the upper triangular part was assumed to be correct and used for further system reliability analysis.

944

Table 4. Weight ratios between the optimal designs obtained using the design methods of interest and the optimal designs

945

obtained using the DAM.

Frame	Proportional loading					Nonproportional loading				
	W_{DAM} (kg)	W_{AEAM} W_{DAM}	W_{AIAM} W_{DAM}	W_{DDM85} W_{DAM}	W_{DDM90} W_{DAM}	W_{DAM} (kg)	W_{AEAM} W_{DAM}	W_{AIAM} W_{DAM}	W_{DDM85} W_{DAM}	W_{DDM90} W_{DAM}
1	1,555	1.000	0.874	0.933	0.874	1,555	1.000	0.874	0.918	0.866
2	5,898	1.000	0.890	0.901	0.890	5,898	1.000	0.890	0.901	0.890
3	956	1.000	1.000	1.030	1.000	956	1.000	1.000	1.030	1.000

4	6,144	1.000	0.786	0.786	0.786	6,144	1.000	0.786	0.786	0.786
5	2,127	1.000	0.819	0.835	0.819	2,100	1.000	0.829	0.840	0.829
6	1,911	1.000	1.000	1.000	1.000	1,911	1.000	1.000	1.000	1.000
7	1,795	1.000	1.000	1.000	1.000	1,795	1.000	1.000	1.000	1.000
8	2,339	1.000	1.000	1.000	1.000	2,339	1.000	1.000	1.000	1.000
9	14,713	1.000	0.756	0.783	0.745	14,713	1.000	0.739	0.783	0.745
10	16,286	1.000	0.769	0.810	0.776	16,286	1.000	0.769	0.810	0.776
11	5,556	0.992	0.817	0.847	0.817	5,428	1.000	0.836	0.847	0.837
12	8,365	0.993	0.739	0.763	0.734	8,365	0.982	0.738	0.763	0.734
13	15,445	1.000	0.744	0.760	0.744	15,445	0.977	0.744	0.726	0.739
14	14,898	0.993	0.717	0.691	0.679	14,668	1.008	0.711	0.689	0.685
15	15,264	0.921	0.781	0.807	0.776	15,264	0.912	0.677	0.757	0.731
16	14,075	0.960	0.784	0.827	0.793	14,075	0.960	0.742	0.765	0.764
17	23,579	1.000	0.748	0.782	0.735	23,579	1.000	0.748	0.721	0.716
18	147,507	1.004	0.817	0.846	0.810	147,507	0.995	0.812	0.811	0.810
19	173,323	0.973	0.887	0.923	0.883	171,247	0.985	0.875	0.934	0.894
20	201,085	0.986	0.857	0.884	0.857	200,891	0.986	0.855	0.885	0.855
21	169,382	0.983	0.833	0.874	0.833	169,382	0.979	0.832	0.874	0.815
22	279,319	0.990	0.849	0.878	0.841	279,319	0.990	0.842	0.872	0.806
μ		0.991	0.839	0.862	0.836		0.990	0.832	0.851	0.831
σ		0.019	0.091	0.091	0.095		0.021	0.099	0.100	0.099
V (%)		1.9	10.9	10.5	11.4		2.1	11.9	11.7	11.9
Min.		0.921	0.717	0.691	0.679		0.912	0.677	0.689	0.685
Max.		1.004	1.000	1.030	1.000		1.008	1.000	1.030	1.000

Table 5. System-level reliability indices of the optimal designs.

Frame	Proportional loading					Nonproportional loading				
	DAM	AEAM	AIAM	DDM85	DDM90	DAM	AEAM	AIAM	DDM85	DDM90
1	3.441	3.441	3.065	3.223	3.065	3.441	3.441	3.065	3.064	2.906
2	3.376	3.376	2.599	3.061	2.599	3.376	3.376	2.599	3.061	2.599
3	3.122	3.122	3.122	3.307	3.122	3.122	3.122	3.122	3.307	3.122
4	5.252	5.252	3.706	3.706	3.706	5.252	5.252	3.706	3.706	3.706
5	3.804	3.804	2.812	3.139	2.812	3.887	3.887	2.812	2.979	2.812
6	3.264	3.264	3.264	3.264	3.264	3.264	3.264	3.264	3.264	3.264
7	2.993	2.993	2.993	2.993	2.993	2.993	2.993	2.993	2.993	2.993
8	3.235	3.235	3.235	3.235	3.235	3.235	3.235	3.235	3.235	3.235
9	4.459	4.459	2.765	3.047	2.639	4.459	4.459	2.559	3.047	2.639
10	3.085	3.085	2.715	3.044	2.816	3.085	3.085	2.715	3.044	2.816
11	3.829	3.732	2.621	3.281	2.621	3.753	3.753	2.613	3.166	2.621
12	3.262	2.821	2.671	2.931	2.671	3.262	2.836	2.668	2.931	2.671
13	4.383	4.383	2.839	3.209	2.839	4.383	4.357	2.839	3.024	2.761
14	5.329	5.381	3.095	3.112	3.044	4.954	5.381	3.103	3.044	2.692
15	4.593	4.565	2.990	3.235	2.985	4.593	4.706	2.838	3.167	2.803
16	4.573	4.290	3.239	3.285	3.217	4.573	4.290	2.786	2.889	2.781
17	3.677	3.677	2.815	3.315	2.807	3.677	3.677	2.815	3.177	2.764
18	3.791	3.650	2.731	3.096	2.695	3.791	3.788	2.738	2.870	2.695
19	2.849	2.706	2.613	2.918	2.568	2.852	2.706	2.521	2.918	2.568
20	3.020	2.948	2.635	2.911	2.635	3.059	2.914	2.668	2.911	2.668
21	3.261	3.123	2.688	2.882	2.658	3.261	3.215	2.681	2.882	2.590
22	3.332	3.329	2.760	2.915	2.713	3.332	3.329	2.737	2.900	2.645
μ	3.724	3.665	2.908	3.141	2.896	3.709	3.685	2.867	3.072	2.834
σ	0.730	0.754	0.283	0.192	0.288	0.692	0.761	0.285	0.192	0.279
V (%)	19.6	20.6	9.7	6.1	9.9	18.7	20.6	9.9	6.3	9.8
Min.	2.849	2.706	2.599	2.882	2.568	2.852	2.706	2.521	2.870	2.568
Max.	5.329	5.381	3.706	3.706	3.706	5.252	5.381	3.706	3.706	3.706

Table 6. Weights, weight ratios, and system-level reliability indices of the optimal designs obtained using the AIAM with the

reduction factor of 0.85 on E and F_y .

Frame	Proportional loading			Nonproportional loading		
	W_{AIAM85} (kg)	$\frac{W_{AIAM85}}{W_{DAM}}$	β_{AIAM85}	W_{AIAM85} (kg)	$\frac{W_{AIAM85}}{W_{DAM}}$	β_{AIAM85}
1	1,451	0.933	3.223	1,451	0.933	3.223
2	5,311	0.901	3.061	5,311	0.901	3.061
3	985	1.030	3.307	985	1.030	3.307
4	4,831	0.786	3.706	4,831	0.786	3.706
5	1,775	0.835	3.139	1,775	0.845	3.139
6	1,911	1.000	3.264	1,911	1.000	3.264
7	1,795	1.000	2.993	1,795	1.000	2.993
8	2,339	1.000	3.235	2,339	1.000	3.235
9	11,517	0.783	3.047	11,517	0.783	2.943
10	13,184	0.810	3.044	13,184	0.810	3.044
11	4,705	0.847	3.281	4,705	0.867	3.281
12	6,696	0.800	3.054	6,477	0.774	3.053
13	12,070	0.781	3.275	11,976	0.775	3.356
14	10,681	0.717	3.095	10,498	0.716	3.312
15	12,350	0.809	3.199	10,826	0.709	3.185
16	11,382	0.809	3.508	10,826	0.769	3.075
17	18,184	0.771	3.330	18,184	0.771	3.330
18	126,778	0.859	3.092	125,673	0.852	3.072
19	160,070	0.924	2.925	159,920	0.934	2.916
20	181,389	0.902	2.917	180,275	0.897	2.903
21	149,668	0.884	2.915	148,697	0.878	2.904
22	250,650	0.897	3.021	249,762	0.894	3.100
μ		0.867	3.165		0.860	3.155
σ		0.087	0.195		0.096	0.191
V (%)		10.0	6.2		11.1	6.0
Min.		0.717	2.915		0.709	2.903
Max.		1.030	3.706		1.030	3.706